A consistent nonlocal scheme based on filters for the homogenization of heterogeneous linear materials with non-separated scales

Julien Yvonnet, Guy Bonnet

HAL Id: hal-00880393
https://hal.science/hal-00880393

Submitted on 7 Sep 2014

A consistent nonlocal scheme based on filters for the homogenization of heterogeneous linear materials with non-separated scales

J. Yvonnet[1] *, G. Bonnet[1] ,

[a1]*Université Paris-Est, Laboratoire Modélisation et Simulation Multi Échelle MSME UMR 8208 CNRS, 5 bd Descartes, F-77454 Marne-la-Vallée, France.*

Abstract

In this work, the question of homogenizing linear elastic, heterogeneous materials with periodic microstructures in the case of non-separated scales is addressed. A framework if proposed, where the notion of mesoscopic strain and stress fields are defined by appropriate integral operators which act as low-pass filters on the fine scale fluctuations. The present theory extends the classical linear homogenization by substituting averaging operators by integral operators, and localization tensors by nonlocal operators involving appropriate Green functions. As a result, the obtained constitutive relationship at the mesoscale appears to be nonlocal. Compared to nonlocal elastic models introduced from a phenomenological point of view, the nonlocal behavior has been fully derived from the study of the microstructure. A discrete version of the theory is presented, where the mesoscopic strain field is approximated as a linear combination of basis functions. It allows computing the mesoscopic nonlocal operator by means of a finite number of transformation tensors, which can be computed numerically on the unit cell.

Key words: Non-separated scales, Homogenization, Coarse-graining, Nonlocal elasticity

1 Introduction

Classical homogenization theory assumes separation between scales, i.e. that the overall strain and stress fields have a characteristic wavelength which is

---

* Correspondance to J. Yvonnet
   Email address: `julien.yvonnet@univ-paris-est.fr` (J. Yvonnet[1]).

much larger than that of the microscopic fluctuations fields. When this assumption is not met, e.g. when the wavelength associated with the applied load is comparable with that of strain and stress fluctuations, the material behavior at a point is influenced by the deformation of neighboring points and the assumption of scale separation is no more valid. In that case, homogenized models able to capture the effects of a non-uniform overall strain are required. In addition, the notion of *mesoscopic models* has recently emerged in the literature. By mesoscopic models, we refer to a description of the behavior halfway between a fully (microscopic) detailed one and a fully homogenized (macroscopic) one using a constant effective tensor. In that sense, mesoscopic models correspond to equivalent behaviors when scales are not separated.

Two main classes of approaches have been proposed in the last decades to model homogenized media when scales are not separated.

The first class of methods uses generalized continuum mechanics by including gradient of strain or higher derivatives of the strain. Generalized continuum mechanics theories have been proposed since the works of Toupin [43], Mindlin [32] and Mindlin and Eshel [33]. These approaches are phenomenological and do not derive from a micromechanical analysis. Furthermore, they require identifying a large number of coefficients associated with higher-order tensors.

In [27], Kouznetsova *et al.* used an extension of the classical computational homogenization techniques to a full geometrically non-linear gradient approach. Macroscopic equations are derived based on the work of Toupin [43] and Koiter [26] for the couple-stress continuum and generalized by Mindlin and Eshel [33], see also [18] for a full gradient variational principle. In [37], Ostoja-Starzewski *et al.* and Bouyge *et al.* [4] have used the unit cell model with a different type of boundary conditions to calculate the overall moduli and characteristic length of a homogenized couple-stress model composed of classically linearly elastic constituents. De Felice and Rizzi [6] and Yuan and Tomita [48] have extended the classical homogenization scheme [41] based on the Hill-Mandel macro homogeneity condition to the Cosserat medium. Other works [4,5,27,28,48] derive the constitutive equations of generalized continuum models through higher-order boundary conditions on the unit cell and use a generalization of the Hill-Mandel condition. As mentioned in Yuan *et al.* [48], these approaches can lead to unphysical results in some situations due to an over-evaluation of the macroscopic internal energy of the medium. In addition, when the cell is homogeneous, the resulting macroscopic behavior remains in some cases a gradient elastic model which is obviously unsatisfying.

In [19] Forest and Sab have proposed a framework to derive an effective linear Cosserat continuum from a heterogeneous classical continuum microscopic model, and from a linear Cosserat microscopic model in [20]. In [21], the asymptotic homogenization method,classically used for periodic heteroge-

neous materials, has been applied to linearly elastic Cosserat microstructural constituents.

In the case of periodic microstructures, Gambin and Kröner, Boutin [23,3], Triantafyllidis and Bardenahgen [46], and Smyshlyaev and Cherednichenko [40] have studied the influence of high-order terms of the series expansion on the macroscopic behavior of linear elastic composites, initiated by Bensoussan *et al.* [1] and Sanchez-Palencia [39]. When the expansion parameter associated with the length ratio is no more small compared to one, then a rigorous framework can be established to introduce the effects of strain and stress gradients on the local response of heterogeneous composites.

Following Boutin [3] and Smyshlyaev and Cherednichenko [40], Tran *et al.* [45] proposed a more systematic framework to define the coefficients of strain gradient elasticity in a series expansion framework. At the microscopic scale the phases are locally elastic but as the separation of scales no more holds, the material obeys strain gradient elasticity. The authors have shown that depending on the truncation order, strain gradient theory of Toupin [43,44], Mindlin [32], Mindlin and Eshel [33], or a general theory of Green and Rivlin [25] can be recovered.

A second class of theories uses nonlocal approaches to model the equivalent homogenized medium. Diener [7–9] and later Drugan and Willis [10] derived a nonlocal constitutive model from the Hashin-Shtrikman variational principle. Other approaches provide a nonlocal constitutive equation relating the mean stress and strain fields [2,47,22]. Luciano and Willis [31] introduced nonlocal constitutive behavior of an infinite laminated composite. The nonlocal elasticity theory can be traced back to Kröner [29,30] who formulated a continuum theory for classical materials with long range cohesive forces. Eringen [11–13], Eringen and Edelen [14] produced nonlocal elasticity theories characterizing the presence of nonlocality residues of fields (like body forces, mass, entropy, internal energy...). Eringen and Kim [15,16] simplified the above mentioned theory for linear homogeneous isotropic nonlocal elastic solids in such a way that the nonlocal theory differs from the classical one in the stress-strain constitutive relations only, with the elastic modulus being a simple function of the Euclidean distance between the strain and stress points. One serious issue is that this theory cannot take into account the presence of cracks or voids in the nonlocal model. In [17] Eringen proposed a differential form to compute the nonlocal operator. However, this model is empirical and does not derive from microstructural considerations. In Gao [24], an asymmetric theory of nonlocal elasticity is provided, and it is shown that the higher gradient model can be deduced from the nonlocal theory. In [38] a thermodynamic and variational framework is proposed in the context of the nonlocal elasticity theory of Eringen [11–13] and provided a nonlocal FEM based methodology as well as a treatment for the presence ofcracks in the nonlocal model by replacing the

Euclidean distance by a geodetical distance. A special mention may be made of nonlocal macroscopic behavior described by using wave-vectors dependent behavior in Fourier domain for conduction [22], which clearly indicates that separation of scale is no more achieved, but without a clear methodology for describing the kernel appearing in the constitutive behavior.

The framework proposed in this study belongs to the second class of theories, i.e. nonlocal approaches. However, compared to numerous previous works based on a phenomenological approach of the macroscopic behavior, a systematic methodology is provided to derive the nonlocal relations of the effective continuum including naturally all the effects of microstructural constituents. The present methodology then defines a *consistent nonlocal homogenization* procedure, without any empirical model. We first define the mesoscopic fields by means of nonlocal smoothing (filters) operators acting on the fine scale fluctuations of the microscopic fields. Then, we introduce a splitting of the strain field into a mesoscopic (filtered) part and the remaining fluctuation. A localization problem can be defined on a unit cell, as a function of the mesoscopic strain field, which appears as a non-uniform eigenstrain. Using an appropriate Green's tensor, the nonlocal mesoscopic constitutive relationship can be derived.

The paper content is as follows. In section 2, the definitions of mesoscopic fields and of the localization problem in the context of non-separated scales are introduced. In section 3, the homogenized quantities are defined, and analogies with classical homogenization are drawn. In section 4, we show that the present theory matches the classical homogenization when the scales are separated, and that we recover classical (local) elastic media when the material is homogeneous. In section 5, a discrete theory is provided, to set the problems to be solved in the unit cell in a numerical context. Guidelines for numerical computations are provided, even though finite element implementation details are left to a separated forthcoming study. Numerical examples are presented in section 6 for illustration.

2 Localization problem for consistent nonlocal homogenization

2.1 Definition of mesoscopic fields through filters

We consider a domain $\Omega \in \mathbb{R}^3$, whose external boundary is denoted by $\partial\Omega$. The material is supposed to be linearly elastic. We assume that the domain Ω is associated with a unit cell of a periodic microstructure characterized by its size whose order is λ and therefore wave-number (or frequency) $\omega = 2\pi/\lambda$. We associate this size to a scale that we call microscopic scale, denoted by $\mathcal{S}$.

Now let us define another scale $\hat{\mathcal{S}}$ related to a characteristic wavelength $\hat{\lambda} > \lambda$ and frequency $\hat{\omega} = 2\pi/\hat{\lambda}$, where $\hat{\lambda}$ is not necessarily much larger compared to λ. This characteristic wavelength is representative of an applied loading (external or body forces) on Ω. We denote by $\hat{\varepsilon}(\mathbf{x})$ and $\hat{\boldsymbol{\sigma}}(\mathbf{x})$ the strain and stress fields related to the scale $\hat{\mathcal{S}}$, called *mesoscopic* strain and stress fields. Similarly to the classical homogenization scheme, this mesoscopic field will induce fluctuations at the scale of the microstructure which will have a wavelength λ. The microscopic strain and stress, resulting in superposition of the applied mesoscopic fields and of the local fluctuations in Ω, are denoted by $\boldsymbol{\varepsilon}(\mathbf{x})$ and $\boldsymbol{\sigma}(\mathbf{x})$, respectively.

In the present work, we consider that mesoscopic fields are related to microscopic ones through appropriate low-pass filters, e.g. by means of a convolution product:

$$\hat{\boldsymbol{\varepsilon}}(\mathbf{x}) = \gamma_\alpha(\mathbf{x}) * \boldsymbol{\varepsilon}(\mathbf{x}) = \int_{\Omega_\infty} \gamma_\alpha(\mathbf{x} - \mathbf{y})\boldsymbol{\varepsilon}(\mathbf{y})d\mathbf{y}, \tag{1}$$

$$\hat{\boldsymbol{\sigma}}(\mathbf{x}) = \gamma_\alpha(\mathbf{x}) * \boldsymbol{\sigma}(\mathbf{x}) = \int_{\Omega_\infty} \gamma_\alpha(\mathbf{x} - \mathbf{y})\boldsymbol{\sigma}(\mathbf{y})d\mathbf{y}, \tag{2}$$

where $d\mathbf{y}$ means that integration is carried out with respect to $\mathbf{y}$, and Ω_∞ is the (convex) infinite domain in which Ω is embedded. These relations express logically that the low-pass filter removes the fluctuations at the small scale. For example, Gaussian filters use a kernel function which can be expressed in one dimension as

$$\gamma_\alpha(x - y) = \frac{1}{\alpha\pi^{1/2}}e^{-\frac{(x-y)^2}{\alpha^2}}, \tag{3}$$

where $\alpha = \sqrt{2}\bar{\sigma}$ is the characteristic length associated with the filter, $\bar{\sigma}$ being the standard deviation of the Gaussian distribution. In higher dimensions, radial forms of (3) can be employed, as well as product of (3) along each direction. Other functions $\gamma_\alpha(\mathbf{x})$ can be chosen, like any other function corresponding to "regularized Dirac delta functions" (bell-shaped, conical [38], etc.) i.e. which satisfy the properties

$$\int_{\Omega_\infty} \gamma_\alpha(\mathbf{x})dx = 1 \tag{4}$$

and

$$\gamma_\alpha(\mathbf{x}) = \delta(\mathbf{x}), \atop \alpha\to 0 \tag{5}$$

where $\delta(\mathbf{x})$ is the Dirac delta function. However, for nonlocal homogenization, the filters are related to values of α which are larger than λ, as seen before. It is worthwhile noticing that the filter being defined by a scalar function, the
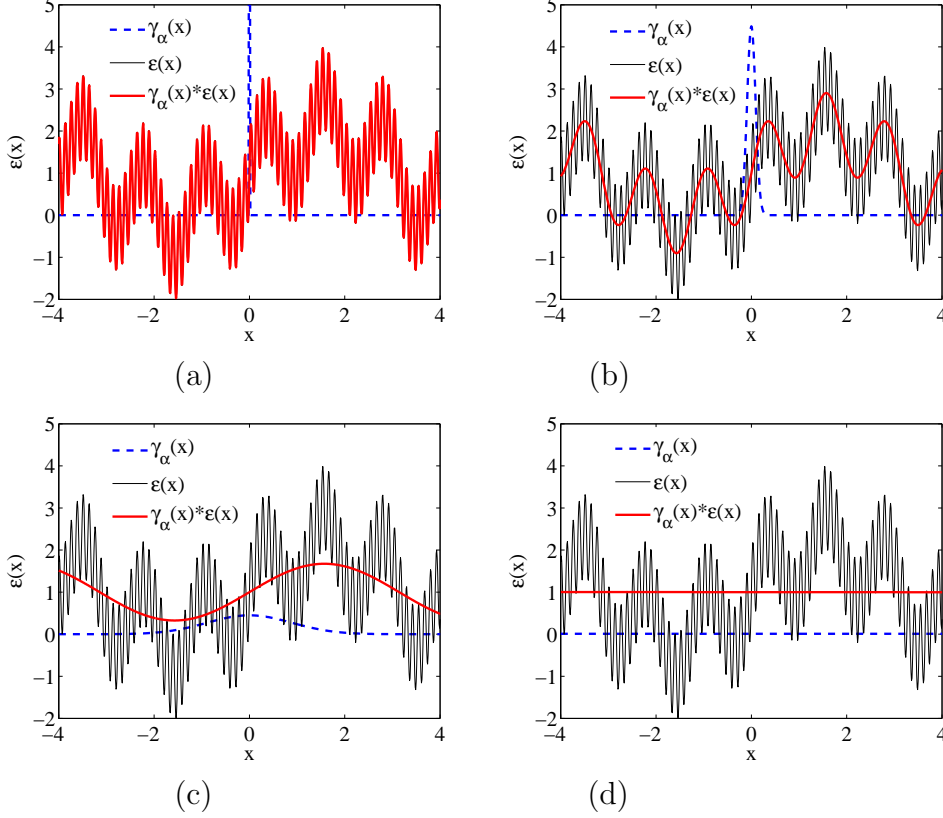
Fig. 1. Action of the filter on an oscillating strain field with characteristic fluctuation length λ_{min}, for different values of the characteristic cut-off wavelength α: a) $\alpha/\lambda_{min} = 1/20$; b) $\alpha/\lambda_{min} = 1$; $\alpha/\lambda_{min} = 20$; $\alpha/\lambda_{min} = 500$.

filtered strain field is compatible and the filtered stress field is equilibrated as soon as there are no body forces. As an example, we depict in figure 1 a microscopic strain field $\varepsilon(x)$, the mesoscopic strain field $\hat{\varepsilon}(x)$ obtained by applying a convolution product with a Gaussian kernel function of the form (3) and different characteristic filter wavelengths, or cut-off wavelengths α. The analytical function used for $\varepsilon(x)$ is $\varepsilon(x) = 1 + sin(50x) + sin(5x) + sin(x)$.

For the sake of clarity, we will omit in the sequel the index α when no confusion is possible, and will simply denote γ_α by γ.

2.2 Localization problem

From the previous considerations, the mesoscopic strain induces rapid microscopic fluctuations having a short wavelength λ, which are denoted $\tilde{\varepsilon}(\mathbf{x})$. The complete strain at the local scale is the superposition of the mesoscopic strain

6

and of the induced fluctuation, leading to:

$$\boldsymbol{\varepsilon}(\mathbf{x}) = \hat{\boldsymbol{\varepsilon}}(\mathbf{x}) + \tilde{\boldsymbol{\varepsilon}}(\mathbf{x}), \tag{6}$$

where $\hat{\boldsymbol{\varepsilon}}(\mathbf{x})$ is the filtered part, or mesoscopic strain field defined by (1) and $\tilde{\boldsymbol{\varepsilon}}(\mathbf{x})$ is a remaining fluctuation due to the presence of heterogeneities. From a practical point of view, the mesoscopic strain field is given, while $\tilde{\boldsymbol{\varepsilon}}(\mathbf{x})$ is the sought local response to this mesoscopic strain field.

We define the following localization problem for nonlocal homogenization, when scales are not separated. Given a non-uniform mesoscopic strain field $\hat{\boldsymbol{\varepsilon}}(\mathbf{x})$, we seek for a compatible strain field $\boldsymbol{\varepsilon}(\mathbf{x})$ such that

$$\nabla \cdot (\mathbb{C}(\mathbf{x}) : \boldsymbol{\varepsilon}(\mathbf{x})) = 0 \quad \text{in } \Omega \tag{7}$$

and

$$\gamma(\mathbf{x}) * \boldsymbol{\varepsilon}(\mathbf{x}) = \hat{\boldsymbol{\varepsilon}}(\mathbf{x}) \quad \text{in } \Omega, \tag{8}$$

where $\mathbb{C}(\mathbf{x})$ is the fourth-order elasticity tensor, assumed known at all points of Ω. As opposed to classical homogenization where it is required that the average of the strain field matches the macroscopic one (see e.g. [42]), the new condition (8) introduced in this work states that the convolution of the local field must match the given non-uniform mesoscopic strain field $\hat{\boldsymbol{\varepsilon}}(\mathbf{x})$. Introducing (6) in (7) we obtain

$$\nabla \cdot (\mathbb{C}(\mathbf{x}) : \tilde{\boldsymbol{\varepsilon}}(\mathbf{x})) = -\nabla \cdot (\mathbb{C}(\mathbf{x}) : \hat{\boldsymbol{\varepsilon}}(\mathbf{x})) \quad \text{in } \Omega, \tag{9}$$

and $\tilde{\boldsymbol{\varepsilon}}(\mathbf{x})$ must satisfy compatibility equations and condition (8). In (9), $\hat{\boldsymbol{\varepsilon}}(\mathbf{x})$ can be interpreted as a non-uniform prescribed eigenstrain. Note that problem (9) with condition (8) is different from the classical homogenization problem. First, $\hat{\boldsymbol{\varepsilon}}(\mathbf{x})$ is generally not Ω-periodic. Second, condition (8) is strongly different from a condition on the average value of $\tilde{\boldsymbol{\varepsilon}}(\mathbf{x})$, as it cannot simply be interpreted as a boundary condition. We propose a solution to enforce this condition in section 2.3.

Assuming that the definition of appropriate boundary conditions leads to a unique solution of the previous problem and due to the linearity of the problem, $\tilde{\boldsymbol{\varepsilon}}(\mathbf{x})$ can be formally expressed by means of an appropriate fourth-order Green's tensor $\hat{\Gamma}$ as

$$\tilde{\boldsymbol{\varepsilon}}(\mathbf{x}) = -\int_{\Omega} \hat{\Gamma}(\mathbf{x}, \mathbf{y}) : \hat{\boldsymbol{\varepsilon}}(\mathbf{y}) d\mathbf{y}, \tag{10}$$

where the definition of the Green's function $\hat{\Gamma}$ is provided in Appendix 8.1.

Using (6) leads to:

$$\varepsilon(\mathbf{x}) = \hat{\varepsilon}(\mathbf{x}) - \int_\Omega \hat{\Gamma}(\mathbf{x}, \mathbf{y}) : \hat{\varepsilon}(\mathbf{y}) d\mathbf{y}, \tag{11}$$

which can also be re-written as

$$\varepsilon(\mathbf{x}) = \int_\Omega \hat{\mathbb{A}}(\mathbf{x}, \mathbf{y}) : \hat{\varepsilon}(\mathbf{y}) d\mathbf{y} \tag{12}$$

with

$$\hat{\mathbb{A}}(\mathbf{x}, \mathbf{y}) = \mathbb{I}\delta(\mathbf{x} - \mathbf{y}) - \hat{\Gamma}(\mathbf{x}, \mathbf{y}), \tag{13}$$

where $\mathbb{I}$ is the fourth-order identity tensor defined by $(I_{ijkl}) = \frac{1}{2}\left(\delta_{ik}\delta_{jl} + \delta_{il}\delta_{jk}\right)$. The local stress is finally obtained from $\hat{\varepsilon}(\mathbf{x})$ as

$$\boldsymbol{\sigma}(\mathbf{x}) = \mathbb{C}(\mathbf{x}) : \int_\Omega \hat{\mathbb{A}}(\mathbf{x}, \mathbf{y}) : \hat{\varepsilon}(\mathbf{y}) d\mathbf{y}. \tag{14}$$

As it can be seen from this last relation, the tensor $\hat{\mathbb{A}}$ allows to find the local strain from the mesoscopic strain. It is therefore the analogous to the localization tensor of the classical homogenization theory. It will be called again localization tensor. However, the main difference with the classical case is that the localization tensor is now a nonlocal operator. The objective of the following subsections is to describe a methodology able at constructing the localization operator.

2.3 Definition of an auxiliary problem and boundary conditions

The previous problem is similar to the classical homogenization problem for separated scales, but the classical methodology cannot be used as soon as the mescoscopic field is not constant. The objective of this section is to present an auxiliary problem involving explicitly the filter for seeking the microscopic contribution of the strain field and define appropriate boundary conditions on the boundary of the unit cell.

2.3.1 A nonlocal cell problem

Let $\mathbf{f}_\alpha(\mathbf{x})$ be a tensor field with a characteristic fluctuation length α. For a Gaussian filter, we have the relation:

$$\gamma(\mathbf{x}) * (\gamma(\mathbf{x}) * \mathbf{f}_\alpha(\mathbf{x})) = h\gamma(\mathbf{x}) * \mathbf{f}_\alpha(\mathbf{x}) \simeq \gamma(\mathbf{x}) * \mathbf{f}_\alpha(\mathbf{x}), \tag{15}$$

where $h = e^{-\alpha^2 \hat{\omega}^2/4}$ is a correction term which is function of the characteristic frequency of the filtered function $\hat{\omega}$ (see details in Appendix 8.2).

Using (6) and applying the convolution product we have

$$\gamma(\mathbf{x}) * \boldsymbol{\varepsilon}(\mathbf{x}) = \gamma(\mathbf{x}) * \hat{\boldsymbol{\varepsilon}}(\mathbf{x}) + \gamma(\mathbf{x}) * \tilde{\boldsymbol{\varepsilon}}(\mathbf{x}). \tag{16}$$

The first right-hand term of Eq. (16) can be approximated from (8) and (15) as

$$\gamma(\mathbf{x}) * \hat{\boldsymbol{\varepsilon}}(\mathbf{x}) = \gamma(\mathbf{x}) * \gamma(\mathbf{x}) * \boldsymbol{\varepsilon}(\mathbf{x}) \simeq h\gamma(\mathbf{x}) * \boldsymbol{\varepsilon}(\mathbf{x}) \approx h\hat{\boldsymbol{\varepsilon}}(\mathbf{x}) \,. \tag{17}$$

Using (16) and (17) we obtain

$$\gamma(\mathbf{x}) * \boldsymbol{\varepsilon}(\mathbf{x}) \simeq h\hat{\boldsymbol{\varepsilon}}(\mathbf{x}) + \gamma(\mathbf{x}) * \tilde{\boldsymbol{\varepsilon}}(\mathbf{x}). \tag{18}$$

Then, condition (8) is satisfied if

$$\gamma(\mathbf{x}) * \tilde{\boldsymbol{\varepsilon}}(\mathbf{x}) \simeq (1 - h)\hat{\boldsymbol{\varepsilon}}(\mathbf{x}). \tag{19}$$

In the case $h \simeq 1$, condition (19) becomes

$$\gamma(\mathbf{x}) * \tilde{\boldsymbol{\varepsilon}}(\mathbf{x}) \simeq 0. \tag{20}$$

Considering the exact condition (19) has been studied and it was found that it would make the definition of the boundary conditions over the RVE much more complicated. As a consequence, assumption $h \simeq 1$ is a key point in the procedure. In the following, we assume that the approximation introduced by (20) is acceptable. To support this assumption, we show some illustration of the associated error in a filter procedure in Appendix 8.2.

One way to verify (20) is to choose $\tilde{\boldsymbol{\varepsilon}}(\mathbf{x})$ such that

$$\tilde{\boldsymbol{\varepsilon}}(\mathbf{x}) = \mathbf{e}(\mathbf{x}) - \gamma(\mathbf{x}) * \mathbf{e}(\mathbf{x}) = \mathbb{W}(\mathbf{x}) * \mathbf{e}(\mathbf{x}) \tag{21}$$

where $\mathbf{e}(\mathbf{x})$ is a new sought compatible strain field that we call auxiliary strain field, and $\mathbb{W}(\mathbf{x}) = \mathbb{I}\delta(\mathbf{x}) - \gamma(\mathbf{x})$. Introducing (21) in (20) and using (15) with $h \simeq 1$ we can verify that

$$\gamma(\mathbf{x}) * (\mathbf{e}(\mathbf{x}) - \gamma(\mathbf{x}) * \mathbf{e}(\mathbf{x})) = \gamma(\mathbf{x}) * \mathbf{e}(\mathbf{x}) - \gamma(\mathbf{x}) * \gamma(\mathbf{x}) * \mathbf{e}(\mathbf{x})$$

$$\simeq \gamma(\mathbf{x}) * \mathbf{e}(\mathbf{x}) - \gamma(\mathbf{x}) * \mathbf{e}(\mathbf{x}) = 0. \tag{22}$$

The localization problem can then be reformulated by seeking for the auxiliary strain $\mathbf{e}(\mathbf{x})$ through:

$$\nabla \cdot (\mathbb{C}(\mathbf{x}) : \mathbb{W}(\mathbf{x}) * \mathbf{e}(\mathbf{x})) = -\nabla \cdot (\mathbb{C}(\mathbf{x}) : \; \hat{\varepsilon}(\mathbf{x})) \quad \text{in } \Omega \tag{23}$$

and

$$\varepsilon(\mathbf{x}) = \hat{\varepsilon}(\mathbf{x}) + \mathbf{e}(\mathbf{x}) - \gamma(\mathbf{x}) * \mathbf{e}(\mathbf{x}). \tag{24}$$

We can verify that (20) implies

$$\langle \tilde{\varepsilon}(\mathbf{x}) \rangle = 0, \tag{25}$$

as $\gamma(\mathbf{x})$ is associated with a low-pass filter. In (25), $\langle . \rangle$ is the spatial average over Ω. Taking the spatial average of Eq. (21) and using (25), we have

$$\langle \mathbf{e}(\mathbf{x}) \rangle - \langle \gamma(\mathbf{x}) * \mathbf{e}(\mathbf{x}) \rangle = 0. \tag{26}$$

As seen from the relation defining the auxiliary strain field $\mathbf{e}(\mathbf{x})$, this one is defined only up to an arbitrary low frequency component, including an arbitrary added constant. This constant can be chosen so as to produce a null average value of the auxiliary field, leading to:

$$\langle \mathbf{e}(\mathbf{x}) \rangle = \mathbf{0}. \tag{27}$$

This condition on $\mathbf{e}(\mathbf{x})$ could be ensured by using a convenient boundary condition on $\partial\Omega$. However, a serious difficulty arises from the presence of the nonlocal operator $\mathbb{W}(\mathbf{x})$ in Eq. (23). To avoid this difficulty, we propose in the following to replace this problem by a cell problem using a local operator.

2.3.2   An associated local cell problem

Let us define the following iterative scheme associated with (23):

$$\nabla \cdot \left(\mathbb{C}(\mathbf{x}) : \mathbf{e}^{k+1}(\mathbf{x}) \right)$$

$$= -\nabla \cdot (\mathbb{C}(\mathbf{x}) : \; \hat{\varepsilon}(\mathbf{x})) + \nabla \cdot \left(\mathbb{C}(\mathbf{x}) : \gamma(\mathbf{x}) * \mathbf{e}^k(\mathbf{x}) \right), \tag{28}$$

where k denotes the iteration index. This iterative scheme is a fixed-point algorithm. Its convergence for any elastic properties is proved in Appendix D. Indeed, it has been observed during all numerical tests that the convergence is achieved. In the following, we use an approximated solution to (23) as the first iteration solution $\mathbf{e}^1(\mathbf{x})$ of (28), with initial solution $\mathbf{e}^0(\mathbf{x}) = 0$, for the

10

sake of simplicity.

Then, the fluctuation is approximated by

$$\tilde{\varepsilon}(\mathbf{x}) \simeq \mathbf{e}^1(\mathbf{x}) - \gamma(\mathbf{x}) * \mathbf{e}^1(\mathbf{x}) \tag{29}$$

where $\mathbf{e}^1(\mathbf{x})$ is the solution of the problem without the nonlocal operator:

$$\nabla \cdot \left(\mathbb{C}(\mathbf{x}) : \mathbf{e}^1(\mathbf{x}) \right) = -\nabla \cdot (\mathbb{C}(\mathbf{x}) : \hat{\varepsilon}(\mathbf{x})) \quad \text{in } \Omega. \tag{30}$$

In addition boundary conditions are applied to enforce that the volume average of $\mathbf{e}^1$ is null, so that:

$$\left\langle \mathbf{e}^1(\mathbf{x}) \right\rangle = \mathbf{0}. \tag{31}$$

In that case, defining a fluctuating displacement $\mathbf{u}^1$ such that $\mathbf{e}^1(\mathbf{x}) = \varepsilon(\mathbf{u}^1(\mathbf{x}))$, where $\varepsilon(.) = \frac{1}{2} \left(\nabla(.) + \nabla^T(.) \right)$, Eq. (31) can be classically expressed as

$$\frac{1}{|\Omega|} \int_\Omega \mathbf{e}^1(\mathbf{x}) d\Omega = \frac{1}{2|\Omega|} \int_{\partial\Omega} \left(\mathbf{u}^1(\mathbf{x}) \otimes \mathbf{n} + \mathbf{n} \otimes \mathbf{u}^1(\mathbf{x}) \right) d\Gamma, \tag{32}$$

where $\mathbf{n}$ is the outward normal to $\partial\Omega$ and $|\Omega|$ the volume of Ω. Eq. (31) is thus satisfied if

$$\mathbf{u}^1(\mathbf{x}) = \mathbf{0} \quad \text{on } \partial\Omega \tag{33}$$

or

$$\mathbf{u}^1(\mathbf{x}) = \tilde{\mathbf{u}}^1(\mathbf{x}) \ , \ \tilde{\mathbf{u}}^1(\mathbf{x}) \text{ periodic on } \Omega. \tag{34}$$

In the present work, the second boundary condition has been adopted for numerical applications.

As a conclusion, given $\hat{\varepsilon}(\mathbf{x})$, finding $\varepsilon(\mathbf{x})$ in Ω requires solving the problem (30) with boundary conditions (33) or (34), and then using (29) to recover the fluctuating strain field, leading finally to the complete local strain by using (6). Obviously, the accuracy of the approximation (29) should depend on the contrast between the phases and on the distribution of local stress. For general contrast and geometries, more than one iteration should be necessary. A related analysis is out of the scope of this paper.

2.3.3 Strain gradient effects

Re-expressing the mesoscopic strain field as

11

$$\hat{\varepsilon}(\mathbf{x}) = \overline{\varepsilon}(\mathbf{x}) + \delta\hat{\varepsilon}(\mathbf{x}) \tag{35}$$

with $\overline{\varepsilon}(\mathbf{x}) = \langle\hat{\varepsilon}(\mathbf{x})\rangle$ and $\delta\hat{\varepsilon}(\mathbf{x}) = \hat{\varepsilon}(\mathbf{x}) - \langle\hat{\varepsilon}(\mathbf{x})\rangle$, the problem (30) yields:

$$\nabla \cdot \left(\mathbb{C}(\mathbf{x}) : \mathbf{e}^1(\mathbf{x})\right) = -\nabla \cdot (\mathbb{C}(\mathbf{x}) : \overline{\varepsilon}(\mathbf{x})) - \nabla \cdot (\mathbb{C}(\mathbf{x}) : \delta\hat{\varepsilon}(\mathbf{x})). \tag{36}$$

It is straightforward to note that when $\delta\hat{\varepsilon}(\mathbf{x}) = 0$ with boundary conditions (33) or (34), then $\mathbf{e}^1(\mathbf{x}) = \tilde{\varepsilon}(\mathbf{x})$ is the strain fluctuation field associated with the classical homogenization problem with separated scales. Then strain gradient effects are induced by the strain field solution of the problem

$$\nabla \cdot (\mathbb{C}(\mathbf{x}) : \delta\mathbf{e}(\mathbf{x})) = -\nabla \cdot (\mathbb{C}(\mathbf{x}) : \delta\hat{\varepsilon}(\mathbf{x})). \tag{37}$$

Note that when $\langle\hat{\varepsilon}(\mathbf{x})\rangle = 0$, $\delta\mathbf{e}(\mathbf{x})$ is zero in the 1D case, as shown in the simple example of Appendix 8.3. However, it is generally nonzero for unit cells defined in two and three dimensions, as illustrated in the numerical examples of section 6.

3   Mesoscopic homogenization

3.1   Mesoscopic constitutive relationships

Using (2) and (14) the mesoscopic stress is expressed by

$$\hat{\boldsymbol{\sigma}}(\mathbf{x}) = \gamma(\mathbf{x}) * \left\{\mathbb{C}(\mathbf{x}) : \int_\Omega \hat{\mathbb{A}}(\mathbf{x}, \mathbf{y}) : \hat{\varepsilon}(\mathbf{y}) d\mathbf{y}\right\} \tag{38}$$

$$= \int_{\Omega_\infty} \int_\Omega \gamma(\mathbf{z})\mathbb{C}(\mathbf{x} - \mathbf{z}) : \hat{\mathbb{A}}(\mathbf{x} - \mathbf{z}, \mathbf{y}) : \hat{\varepsilon}(\mathbf{y}) d\mathbf{y} d\mathbf{z}. \tag{39}$$

Setting $\mathbf{t} = \mathbf{x} - \mathbf{z}$, $d\mathbf{t} = -d\mathbf{z}$, then the integral in (39) is equal to

$$\int_\Omega \int_{\Omega_\infty} \gamma(\mathbf{x} - \mathbf{t})\mathbb{C}(\mathbf{t}) : \hat{\mathbb{A}}(\mathbf{t}, \mathbf{y}) : \hat{\varepsilon}(\mathbf{y}) d\mathbf{y} d\mathbf{t}. \tag{40}$$

We finally obtain

$$\hat{\boldsymbol{\sigma}}(\mathbf{x}) = \int_\Omega \hat{\mathbb{C}}(\mathbf{x}, \mathbf{y}) : \hat{\varepsilon}(\mathbf{y}) d\mathbf{y}, \tag{41}$$

with

$$\hat{\mathbb{C}}(\mathbf{x}, \mathbf{y}) = \int_{\Omega_\infty} \gamma(\mathbf{x} - \mathbf{t})\mathbb{C}(\mathbf{t}) : \hat{\mathbb{A}}(\mathbf{t}, \mathbf{y}) d\mathbf{t} = \gamma(\mathbf{x}) * \{\mathbb{C}(\mathbf{x}) : \mathbb{A}(\mathbf{x}, \mathbf{y})\}.$$

The constitutive law (41) defines a nonlocal constitutive relationship between $\hat{\boldsymbol{\sigma}}(\mathbf{x})$ and $\hat{\boldsymbol{\varepsilon}}(\mathbf{x})$ which describes the behavior at the mesoscopic scale $\hat{\mathcal{S}}$.

The mesoscopic potential energy can be expressed as

$$\Pi(\hat{\boldsymbol{\varepsilon}}(\mathbf{x})) = \frac{1}{2} \int_{\Omega_\infty} \int_\Omega \hat{\mathbb{C}}(\mathbf{x},\mathbf{y}) : \hat{\boldsymbol{\varepsilon}}(\mathbf{x}) : \hat{\boldsymbol{\varepsilon}}(\mathbf{y}) d\mathbf{x} d\mathbf{y} = \int_{\Omega_\infty} W(\hat{\boldsymbol{\varepsilon}}(\mathbf{x})) d\Omega, \quad (42)$$

which is an expression similar to that provided by Polizzotto in [38] in the context of the Eringen model. The main difference with the present model is that the nonlocal operator is here not translation-invariant, i.e. $\hat{\mathbb{C}}(\mathbf{x},\mathbf{y}) \neq \hat{\mathbb{C}}(\mathbf{x}-\mathbf{y})$.

The constitutive equation is then recovered as

$$\hat{\boldsymbol{\sigma}}(\mathbf{x}) = \frac{\partial W(\mathbf{x})}{\partial \hat{\boldsymbol{\varepsilon}}(\mathbf{x})} = \int_\Omega \hat{\mathbb{C}}(\mathbf{x},\mathbf{y}) : \hat{\boldsymbol{\varepsilon}}(\mathbf{y}) d\mathbf{y} \qquad (43)$$

which matches relation (41).

At the scale $\hat{\mathcal{S}}$, we can then define a boundary value problem for the mesoscopic strain field $\hat{\boldsymbol{\varepsilon}}(\mathbf{x})$. Let $W \in \mathbb{R}^3$ be a domain associated with a structure. The equilibrium equation is given by

$$\nabla \cdot (\hat{\boldsymbol{\sigma}}(\mathbf{x})) = 0 \ \ \text{in } W, \qquad (44)$$

where $\hat{\boldsymbol{\sigma}}(\mathbf{x})$ is related to $\hat{\boldsymbol{\varepsilon}}(\mathbf{x})$ through (41). The problem is to find the mesoscopic displacement field $\hat{\mathbf{u}}(\mathbf{x})$ such that $\hat{\boldsymbol{\varepsilon}}(\mathbf{x}) = \boldsymbol{\varepsilon}(\hat{\mathbf{u}}(\mathbf{x}))$ in W satisfying (44) and (41), completed with appropriate Neumann and Dirichlet conditions on the boundary of W.

3.2   Stress formulation and analogies between classical and consistent nonlocal homogenization schemes

A dual problem of (7)-(8) can be stated as follows:

Given a mesoscopic stress field $\hat{\boldsymbol{\sigma}}(\mathbf{x})$, find $\hat{\boldsymbol{\varepsilon}}(\mathbf{x})$ such that (7) is verified and

$$\gamma(\mathbf{x}) * \boldsymbol{\sigma}(\mathbf{x}) = \hat{\boldsymbol{\sigma}}(\mathbf{x}). \qquad (45)$$

Using arguments similar to those of the previous section, we define the following splitting of the stress into mesoscopic and fluctuating parts as

$$\boldsymbol{\sigma}(\mathbf{x}) = \hat{\boldsymbol{\sigma}}(\mathbf{x}) + \tilde{\boldsymbol{\sigma}}(\mathbf{x}). \qquad (46)$$

Then we can formally relate $\tilde{\boldsymbol{\sigma}}(\mathbf{x})$ to $\hat{\boldsymbol{\sigma}}(\mathbf{x})$ by means of an appropriate fourth-order Green's tensor $\hat{\boldsymbol{\Delta}}(\mathbf{x})$

as

$$\tilde{\boldsymbol{\sigma}}(\mathbf{x}) = -\int_{\Omega} \hat{\boldsymbol{\Delta}}(\mathbf{x}, \mathbf{y}) : \hat{\boldsymbol{\sigma}}(\mathbf{y}) d\mathbf{y}. \tag{47}$$

We can express the (total) local stress by

$$\boldsymbol{\sigma}(\mathbf{x}) = \int_{\Omega} \hat{\mathbb{B}}(\mathbf{x}, \mathbf{y}) : \hat{\boldsymbol{\sigma}}(\mathbf{y}) d\mathbf{y}, \tag{48}$$

with

$$\hat{\mathbb{B}}(\mathbf{x}, \mathbf{y}) = \mathbb{I}\delta(\mathbf{x} - \mathbf{y}) - \hat{\boldsymbol{\Delta}}(\mathbf{x}, \mathbf{y}). \tag{49}$$

The strain is thus obtained as

$$\boldsymbol{\varepsilon}(\mathbf{x}) = \mathbb{S}(\mathbf{x}) : \int_{\Omega} \hat{\mathbb{B}}(\mathbf{x}, \mathbf{y}) : \hat{\boldsymbol{\sigma}}(\mathbf{y}) d\mathbf{y}, \tag{50}$$

where $\mathbb{S}(\mathbf{x}) = \mathbb{C}^{-1}(\mathbf{x})$ is the compliance tensor. We can verify that $\gamma(\mathbf{x}) * \tilde{\boldsymbol{\sigma}}(\mathbf{x}) = 0$ implies that

$$\langle \tilde{\boldsymbol{\sigma}}(\mathbf{x}) \rangle = 0. \tag{51}$$

Defining an auxiliary stress field $\mathbf{s}(\mathbf{x})$ such that

$$\tilde{\boldsymbol{\sigma}}(\mathbf{x}) = \mathbf{s}(\mathbf{x}) - \gamma(\mathbf{x}) * \mathbf{s}(\mathbf{x}), \tag{52}$$

Eq. (51) is verified if

$$\langle \mathbf{s}(\mathbf{x}) \rangle - \langle \gamma(\mathbf{x}) * \mathbf{s}(\mathbf{x}) \rangle = 0, \tag{53}$$

or, as discussed previously in section 2.3.2:

$$\langle \mathbf{s}(\mathbf{x}) \rangle = 0, \tag{54}$$

Condition (54) is classically verified by prescribing the following boundary conditions on the elementary cell

$$\mathbf{s}(\mathbf{x})\mathbf{n} = \mathbf{0} \quad \text{on} \quad \partial\Omega. \tag{55}$$

Furthermore, using similar arguments as those of section 3.1, we can establish

the relationship

$$\hat{\boldsymbol{\varepsilon}}(\mathbf{x}) = \int_{\Omega} \hat{\mathbb{S}}(\mathbf{x}, \mathbf{y}) : \hat{\boldsymbol{\sigma}}(\mathbf{y}) d\mathbf{y} \tag{56}$$

with

$$\hat{\mathbb{S}}(\mathbf{x}, \mathbf{y}) = \gamma(\mathbf{x}) * \{\mathbb{S}(\mathbf{x}) : \mathbb{B}(\mathbf{x}, \mathbf{y})\} . \tag{57}$$

Finally, considering relationships (41) and (56), we can conclude that the integral operators with kernel functions $\hat{\mathbb{C}}(\mathbf{x}, \mathbf{y})$ and $\hat{\mathbb{S}}(\mathbf{x}, \mathbf{y})$ are inverse of each other in the sense of linear integral operators.

In Table 1, we summarize relationships of both classical homogenization and the present consistent nonlocal homogenization framework.

Table 1
Summary of relationships for homogenization with separated and non-separated scales.

Classical homogenization with separated scales	Consistent nonlocal homogenization with non-separated scales
Local Constitutive relationships	
$\boldsymbol{\sigma}(\mathbf{x}) = \mathbb{C}(\mathbf{x}) : \boldsymbol{\varepsilon}(\mathbf{x})$	$\boldsymbol{\sigma}(\mathbf{x}) = \mathbb{C}(\mathbf{x}) : \boldsymbol{\varepsilon}(\mathbf{x})$
$\boldsymbol{\varepsilon}(\mathbf{x}) = \mathbb{S}(\mathbf{x}) : \boldsymbol{\sigma}(\mathbf{x})$	$\boldsymbol{\varepsilon}(\mathbf{x}) = \mathbb{S}(\mathbf{x}) : \boldsymbol{\sigma}(\mathbf{x})$
Localization rules	
$\boldsymbol{\varepsilon}(\mathbf{x}) = \mathbb{A}(\mathbf{x}) : \overline{\boldsymbol{\varepsilon}}$	$\boldsymbol{\varepsilon}(\mathbf{x}) = \int_{\Omega} \hat{\mathbb{A}}(\mathbf{x}, \mathbf{y}) : \hat{\boldsymbol{\varepsilon}}(\mathbf{y}) d\Omega$
$\boldsymbol{\sigma}(\mathbf{x}) = \mathbb{B}(\mathbf{x}) : \overline{\boldsymbol{\sigma}}$	$\boldsymbol{\sigma}(\mathbf{x}) = \int_{\Omega} \hat{\mathbb{B}}(\mathbf{x}, \mathbf{y}) : \hat{\boldsymbol{\sigma}}(\mathbf{y}) d\Omega$
Definition of homogenized quantities	
$\overline{\boldsymbol{\varepsilon}} = \langle \boldsymbol{\varepsilon}(\mathbf{x}) \rangle$	$\hat{\boldsymbol{\varepsilon}}(\mathbf{x}) = \gamma(\mathbf{x}) * \boldsymbol{\varepsilon}(\mathbf{x})$
$\overline{\boldsymbol{\sigma}} = \langle \boldsymbol{\sigma}(\mathbf{x}) \rangle$	$\hat{\boldsymbol{\sigma}}(\mathbf{x}) = \gamma(\mathbf{x}) * \boldsymbol{\sigma}(\mathbf{x})$
Effective constitutive relationships	
$\overline{\boldsymbol{\sigma}} = \overline{\mathbb{C}} : \overline{\boldsymbol{\varepsilon}}$	$\hat{\boldsymbol{\sigma}}(\mathbf{x}) = \int_{\Omega} \hat{\mathbb{C}}(\mathbf{x}, \mathbf{y}) : \hat{\boldsymbol{\varepsilon}}(\mathbf{y}) d\Omega$
$\overline{\boldsymbol{\varepsilon}} = \overline{\mathbb{S}} : \overline{\boldsymbol{\sigma}}$	$\hat{\boldsymbol{\varepsilon}}(\mathbf{x}) = \int_{\Omega} \hat{\mathbb{S}}(\mathbf{x}, \mathbf{y}) : \hat{\boldsymbol{\sigma}}(\mathbf{y}) d\Omega$
Effective moduli	
$\overline{\mathbb{C}} = \langle \mathbb{C}(\mathbf{x}) : \mathbb{A}(\mathbf{x}) \rangle$	$\hat{\mathbb{C}}(\mathbf{x}, \mathbf{y}) = \gamma(\mathbf{x}) * \left\{ \mathbb{C}(\mathbf{x}) : \hat{\mathbb{A}}(\mathbf{x}, \mathbf{y}) \right\}$
$\overline{\mathbb{S}} = \langle \mathbb{S}(\mathbf{x}) : \mathbb{B}(\mathbf{x}) \rangle$	$\hat{\mathbb{S}}(\mathbf{x}, \mathbf{y}) = \gamma(\mathbf{x}) * \left\{ \mathbb{S}(\mathbf{x}) : \hat{\mathbb{B}}(\mathbf{x}, \mathbf{y}) \right\}$

It is worth noting that we recover the relationships of classical homogenization by substituting the averaging operator by the nonlocal convolution operator and localization tensors by the appropriate integral operators involving Green's functions. Then the present framework constitutes a consistent extension of classical homogenization to non-separated scales, as detailed in the next section. To our knowledge, such an extension is presented here for the

first time.

4 Case of separated scales and homogeneous media

4.1 Case of separated scales

In the following, we show that when the scales are separated, i.e. when $\alpha >> \lambda$, we recover the classical homogenized quantities and the effective elasticity tensor. Taking again the example of the Gaussian filter, it can be shown that when α tends to infinity, the application of the Gaussian filter recovers the volume average,

$$\gamma_\alpha * (.) \rightarrow \langle . \rangle . \tag{58}$$

This can be shown from a simple one-dimensional example: for $\gamma_\alpha(\mathbf{x})$ of the form (3) and for the oscillating function $f(x) = \langle f \rangle + e^{i\hat{\omega}x}$, the exact expression of the convolution product with $\gamma_\alpha(x)$ is equal to $\gamma_\alpha(x) * f(x) = \langle f \rangle + e^{i\hat{\omega}x - \frac{1}{4}\alpha^2\hat{\omega}^2}$. Then taking the limit $\alpha \rightarrow \infty$, the expression reduces to $\langle f \rangle$ and the mesoscopic strain $\hat{\varepsilon}(\mathbf{x})$ reduces to a constant strain equal to $\langle \varepsilon(\mathbf{x}) \rangle = \overline{\varepsilon}$. Relation (6) then becomes

$$\varepsilon(\mathbf{x}) = \overline{\varepsilon} + \tilde{\varepsilon}(\mathbf{x}) \tag{59}$$

which is the classical splitting of the strain when considering separated scales (see e.g. [42]). Then problem (7)-(8) reduces to the classical localization problem, governed by Eq. (7) with the condition

$$\langle \varepsilon(\mathbf{x}) \rangle = \overline{\varepsilon}. \tag{60}$$

In addition, Eq. (10) yields in that case:

$$\tilde{\varepsilon}(\mathbf{x}) = (\mathbb{I} - \mathbb{A}(\mathbf{x})) : \overline{\varepsilon}, \tag{61}$$

where $\mathbb{A}(\mathbf{x})$ is the classical fourth-order localization tensor such that

$$\varepsilon(\mathbf{x}) = \mathbb{A}(\mathbf{x}) : \overline{\varepsilon}. \tag{62}$$

We finally obtain the classical homogenization relations for separated scales:

$$\boldsymbol{\sigma}(\mathbf{x}) = \overline{\boldsymbol{\sigma}} = \langle \mathbb{C}(\mathbf{x}) : \mathbb{A}(\mathbf{x}) \rangle : \overline{\varepsilon} \tag{63}$$

and

$$\hat{\mathbb{C}} = \overline{\mathbb{C}} = \langle \mathbb{C}(\mathbf{x}) : \mathbb{A}(\mathbf{x}) \rangle . \tag{64}$$

4.2 Case of a homogeneous media

As discussed in the introduction, one serious issue in approaches employing higher-order boundary conditions is that when the volume fraction of heterogeneities in the unit cell tends to zero, the homogeneous media remains a gradient media, which is not satisfactory. In what follows, we show that the present nonlocal model yields a classical local elastic model in the case of a homogeneous media, i.e. for

$$\mathbb{C}(\mathbf{x}) = \mathbb{C}^0, \tag{65}$$

with $\mathbb{C}^0$ a constant elastic tensor. In that situation, the fluctuation $\tilde{\boldsymbol{\varepsilon}}(\mathbf{x})$ vanishes, as well as the Green operator $\hat{\Gamma}(\mathbf{x}, \mathbf{y})$ in (13). Then $\hat{\mathbb{A}}(\mathbf{x}, \mathbf{y})$ reduces to:

$$\mathbb{A}(\mathbf{x}, \mathbf{y}) = \mathbb{I}\delta(\mathbf{x} - \mathbf{y}). \tag{66}$$

From (12), we obtain that in a homogeneous media, then

$$\boldsymbol{\varepsilon}(\mathbf{x}) = \hat{\boldsymbol{\varepsilon}}(\mathbf{x}). \tag{67}$$

Finally, Introducing (66) and (65) in (3.1), we recover the classical local behavior of an elastic media as

$$\hat{\boldsymbol{\sigma}}(\mathbf{x}) = \mathbb{C}^0 : \hat{\boldsymbol{\varepsilon}}(\mathbf{x}). \tag{68}$$

5 Construction of the localization tensor through a discrete formulation

As seen in section 2, the main objective of the present nonlocal homogenization method is to provide the localization tensor which allows to produce the local strain within a periodic cell from the applied mesoscopic strain. The objective of this section is now to provide practical means for providing the mesoscopic localization tensor.

In the general case, it is not possible to obtain a closed-form for the Green's tensor $\hat{\Gamma}$ introduced in Eq. (10). So, a numerical implementation of the compu-

17

tation of the Green's tensor will be performed by using approximate solutions obtained by finite elements. If the fluctuation length $\hat{\lambda}$ associated with the scale $\hat{\mathcal{S}}$ is larger than the microscopic wavelength λ, we can approximate $\hat{\varepsilon}(\mathbf{x})$ by using a small number of orthonormal basis functions $M_p(\mathbf{x})$ with characteristic fluctuation length $\hat{\lambda}$ as

$$\hat{\varepsilon}(\mathbf{x}) \approx \sum_p M_p(\mathbf{x})\hat{\varepsilon}^p, \tag{69}$$

where $\hat{\varepsilon}^p$ are coefficients related to the value of the mesoscopic strain at some points of a coarse meshing at the mesoscopic scale. Several choices are possible for these basis functions, like finite element shape functions on a coarser grid, polynomial basis, etc.

In that case, from the linearity of (23) and using the superposition principle, we can express $\mathbf{e}(\mathbf{x})$ as a sum of fourth-order transformation tensors $\boldsymbol{\Psi}^p(\mathbf{x})$ as

$$e_{ij}(\mathbf{x}) = \sum_p \Psi^p_{ijkl}(\mathbf{x})\hat{\varepsilon}^p_{kl} \tag{70}$$

where $\boldsymbol{\Psi}^p(\mathbf{x})$ could be obtained by solving the following nonlocal problem on a fine grid:

$$\nabla \cdot \left(\mathbb{C}(\mathbf{x}) : \mathbb{W}(\mathbf{x}) * \mathbf{e}^{p,(kl)}(\mathbf{x}) \right) = -\nabla \cdot \left(\mathbb{C}(\mathbf{x}) : \boldsymbol{\chi}^{p,(kl)}(\mathbf{x}) \right) \tag{71}$$

with boundary conditions (33) or (34) and where $\boldsymbol{\chi}^{p,(kl)}(\mathbf{x})$ is a non-uniform eigenstrain prescribed over the support of $M^p(\mathbf{x})$ and defined as

$$\boldsymbol{\chi}^{p,(kl)}(\mathbf{x}) = \frac{M^p(\mathbf{x})}{2} \left(\mathbf{a}_k \otimes \mathbf{a}_l + \mathbf{a}_l \otimes \mathbf{a}_k \right), \tag{72}$$

where $\mathbf{a}_i$ are the base vectors of Cartesian coordinate system and where the transformation tensors are deduced from

$$\Psi^p_{ijkl}(\mathbf{x}) = e^{p,(kl)}_{ij}(\mathbf{x}). \tag{73}$$

As seen before, this nonlocal problem cannot be easily solved by usual means, so we resort to the local problem (30) to approximate $\mathbf{e}^1$. We set $\mathbf{e}^1 = \boldsymbol{\beta}$ so as to avoid heavy notations. From (29) and (71) we have

$$\tilde{\varepsilon}(\mathbf{x}) \simeq \boldsymbol{\beta}^{p,(kl)}(\mathbf{x}) - \gamma(\mathbf{x}) * \boldsymbol{\beta}^{p,(kl)}(\mathbf{x}). \tag{74}$$

where $\boldsymbol{\beta}^{p,(kl)}(\mathbf{x})$ is obtained by solving the problem without the nonlocal operator:

$$\nabla \cdot \left(\mathbb{C}(\mathbf{x}) : \boldsymbol{\beta}^{p,(kl)}(\mathbf{x}) \right) = -\nabla \cdot \left(\mathbb{C}(\mathbf{x}) : \boldsymbol{\chi}^{p,(kl)}(\mathbf{x}) \right) \tag{75}$$

with boundary conditions

$$\mathbf{u}^{\beta}(\mathbf{x}) = \tilde{\mathbf{u}}^{\beta}(\mathbf{x}) \quad on \; \partial\Omega, \tag{76}$$

where $\mathbf{u}^{\beta}$ are the displacements such that $\boldsymbol{\beta}(\mathbf{x}) = \boldsymbol{\varepsilon}(\mathbf{u}^{\beta})$ and $\tilde{\mathbf{u}}^{\beta}(\mathbf{x})$ is a periodic function over Ω.

Then

$$\boldsymbol{\beta}(\mathbf{x}) = \sum_{p} \boldsymbol{\Psi}^{p}(\mathbf{x}) : \hat{\boldsymbol{\varepsilon}}^{p} \tag{77}$$

with

$$\Psi^{p}_{ijkl}(\mathbf{x}) = \beta^{p,(kl)}_{ij}(\mathbf{x}). \tag{78}$$

Then from (74) we can write

$$\tilde{\boldsymbol{\varepsilon}}(\mathbf{x}) \simeq \sum_{p} \boldsymbol{\Psi}^{p}(\mathbf{x}) : \hat{\boldsymbol{\varepsilon}}^{p} - \sum_{p} \gamma(\mathbf{x}) * \boldsymbol{\Psi}^{p}(\mathbf{x}) : \hat{\boldsymbol{\varepsilon}}^{p}. \tag{79}$$

Finally, from (6) and (79) we can express $\boldsymbol{\varepsilon}(\mathbf{x})$ as

$$\boldsymbol{\varepsilon}(\mathbf{x}) = \sum_{p} \hat{\mathbb{A}}^{p}(\mathbf{x}) : \hat{\boldsymbol{\varepsilon}}^{p} \tag{80}$$

with

$$\hat{A}^{p}_{ijkl}(\mathbf{x}) = I_{ijkl} M^{p}(\mathbf{x}) + \Psi^{p}_{ijkl}(\mathbf{x}) - \gamma(\mathbf{x}) * \Psi^{p}_{ijkl}(\mathbf{x}). \tag{81}$$

This last relation achieves the production of the localization tensor $\mathbb{A}$. As seen in the previous section, this tensor relates the local strain to any mesoscopic strain. However, as the mesoscopic strains are built on a discrete space, the nonlocal aspect of the localization operator is displayed through the discrete sum on p, which plays therefore the role of variable $\mathbf{y}$ in the previous section.

Then, the local stress tensor is given by

$$\boldsymbol{\sigma}(\mathbf{x}) = \sum_{p} \mathbb{C}(\mathbf{x}) : \hat{\mathbb{A}}^{p}(\mathbf{x}) : \hat{\boldsymbol{\varepsilon}}^{p}. \tag{82}$$

Finally we obtain the discrete nonlocal constitutive law as

$$\hat{\boldsymbol{\sigma}}(\mathbf{x}) = \sum_{p} \hat{\mathbb{C}}^{p}(\mathbf{x}) : \hat{\boldsymbol{\varepsilon}}^{p} \tag{83}$$

19

where $\hat{\mathbb{C}}^p(\mathbf{x})$ are tensor fields defined over Ω as

$$\hat{\mathbb{C}}^p(\mathbf{x}) = \gamma(\mathbf{x}) * \left\{ \mathbb{C}(\mathbf{x}) : \hat{\mathbb{A}}^p(\mathbf{x}) \right\}. \tag{84}$$

The construction of the nonlocal mesoscopic constitutive law requires therefore the computation of the tensors $\hat{\mathbb{C}}^p(\mathbf{x})$. Having computed these tensors, computing the mesoscopic stress at any point for any given mesoscopic strain requires the projection of the mesoscopic strain tensor on the discrete base followed by the summation of the operators using (83).

6   Numerical examples

The description of the discrete solution of the mesoscopic homogenization is the production of tensors $\hat{\mathbb{A}}^p(\mathbf{x})$, and $\hat{\mathbb{C}}^p(\mathbf{x})$. In the following applications, these tensors will be computed numerically. Several numerical methods can be envisaged, like FEM, XFEM [35], FFT-based methods [36], etc. In the present work, the following choices have been made for the numerical computations. First, the basis functions $M_p(\mathbf{x})$ have been chosen as bilinear finite element shape functions associated to the nodes of a coarse grid composed of a 4×4 quadrilateral elements mesh defined on Ω. Then the local problem (75) - (76) has been solved by the finite element method on a fine regular mesh of quadrilateral elements where all local properties are defined in the elements. The convolution product (1) has been evaluated numerically by approximating the integral as a finite sum and by replacing Ω_∞ by Ω_E, a large domain embedding Ω. For this purpose, a supercell made of 3×3 domains Ω was defined for the integration purpose.

The different steps of the numerical calculations are summarized as follows:

(1) Computation of the nonlocal tensors $\hat{\mathbb{A}}^p(\mathbf{x})$. For each elementary eigenstrain field (72), solve the problem (75) with boundary conditions (76). Then $\hat{\mathbb{A}}^p(\mathbf{x})$ can be computed from (81).
(2) Computation of the nonlocal constitutive tensors $\hat{\mathbb{C}}^p(\mathbf{x})$. For each tensor $\hat{\mathbb{A}}^p(\mathbf{x})$, compute $\hat{\mathbb{C}}^p(\mathbf{x})$ from (84).
(3) Reconstruction of the local response to a given mesoscopic strain field $\hat{\boldsymbol{\varepsilon}}(\mathbf{x})$. The mesoscopic strain field being defined by its discrete values $\hat{\boldsymbol{\varepsilon}}^p$ at the nodes of the coarse grid, the local recovered strain and stress fields $\boldsymbol{\varepsilon}(\mathbf{x})$ and $\boldsymbol{\sigma}(\mathbf{x})$ can be computed from (80) and (82), respectively.
(4) A comparison (reference) solution can be obtained by solving the problem (30) with boundary conditions (34), for $\hat{\boldsymbol{\varepsilon}}(\mathbf{x})$ defined at all integration points of the fine mesh.

20

Several examples will be reported thereafter: in section 6.1, local and filtered (mesoscopic) distributions of strain and stress obtained from step 3 are compared. In section 6.2, the localization tensors computed on a unit cell are used to compute the local response in a structure submitted to a non-uniform mesoscopic strain field.

6.1 Non-uniform mesoscopic strain field in an elementary cell

In this first example, we solve the localization problem on a unit cell and compute the discrete localization and homogenized operators $\mathbb{A}^p(\mathbf{x})$ and $\hat{\mathbb{C}}^p(\mathbf{x})$. Then we apply different mesoscopic strain fields, possibly non-uniform, on the unit cell. The objectives are to check: i) that we can accurately reconstruct the local fields, for an arbitrary given non-uniform mesoscopic strain field; ii) that applying the filter on the equilibrated strain field, we recover the applied mesoscopic strain field, corresponding to condition (8).

The chosen microstructure is described in figure 2, and is composed of 5×5 circular inclusions positioned on a regular lattice in a square domain with volume fraction $f = 0.3$. Even though the microstructure is periodic, we construct a microstructure composed of several inclusions to better appreciate the regularization effects over several heterogeneities. Another reason is that the Gaussian filter induces some boundary effects, which are evidenced in the following numerical examples.

Material properties of the phases are taken as $\lambda_{inc} = \mu_{inc} = 10$ GPa and $\lambda_{mat} = \mu_{mat} = 1$ GPa, where $\lambda_{inc}, \mu_{inc}, \lambda_{mat}$ and μ_{mat} denote the Lamé's parameters of the inclusion and of the matrix, respectively. The mesh related to the fine scale consists of 120×120 - 4 nodes elements. The parameter α of the filter is chosen as $\alpha = \frac{2L}{3N_{inc}}$, where $N_{inc} = 5$ is the number of heterogeneities along one direction. The length is chosen as $L = 120$.

We first prescribe a constant mesoscopic field $\hat{\boldsymbol{\varepsilon}}(\mathbf{x}) = \mathbf{a}_1 \otimes \mathbf{a}_1$. In figure 3, we depict the local field $\varepsilon_{11}(\mathbf{x})$, its reconstruction through (80) and the applied mesoscopic strain field $\hat{\varepsilon}_{11}(\mathbf{x})$ (here matching the macroscopic one) defined on the nodes of the coarse grid and the strain field. For comparison, we also plot the reconstructed mesoscopic field $\gamma(\mathbf{x}) * \varepsilon_{11}(\mathbf{x})$. In this case, as described in section 4, the present theory matches the case of separated scales. We can then check that our scheme correctly reproduces local and global fields in the case of a constant applied strain field.

In a second test, we now apply a linear mesoscopic strain field $\hat{\boldsymbol{\varepsilon}}(\mathbf{x}) = x\mathbf{a}_2 \otimes \mathbf{a}_2$. We compare the different local, mesoscopic, computed and reconstructed strain and stress fields in figures 4 and 5. Note that the two following examples have been chosen such that $\langle \hat{\varepsilon}(\mathbf{x}) \rangle = 0$, to show that the present nonlocal
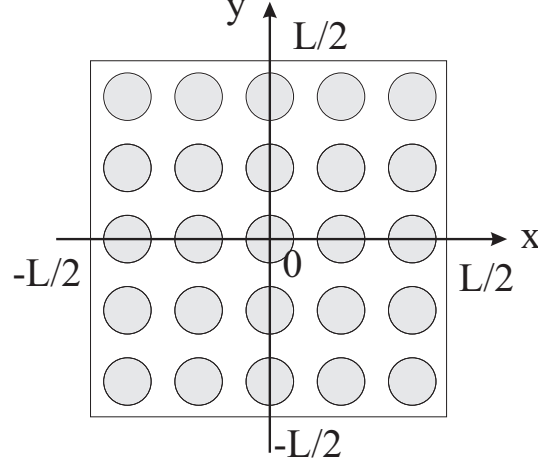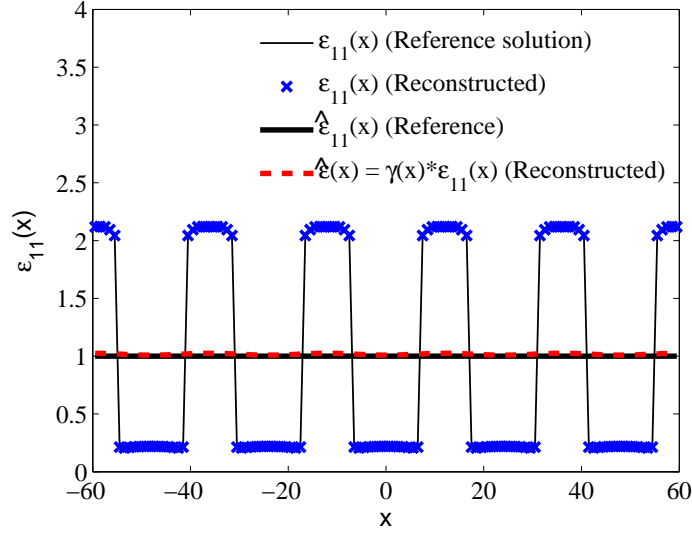
Fig. 2. Elementary cell.

Fig. 3. Elementary cell submitted to a constant mesoscopic strain field. Comparison of local strain fields through a line $(x, y = 0)$ passing through the inclusions.

framework captures high-order strain gradient effects as compared to the classical homogenization scheme.

We can note in figure 4 that away from boundaries of the unit cell, condition (8) is verified with a good accuracy. However, near boundaries, some perturbations occur. These perturbations are a consequence of the numerical method used to compute the Gaussian filter. If the computed local field is discontinuous on two opposite points of $\partial\Omega$, then the Gaussian filter regularizes this discontinuity over the unit cell period. One solution is to use a super-cell composed of several elementary cell, and to compute the solution away from the boundaries where these spurious effects occur. Further improvements will require investigating alternative regularization methodologies which avoid these spurious effects and which would allow using a single cell in the case of a periodic composite.
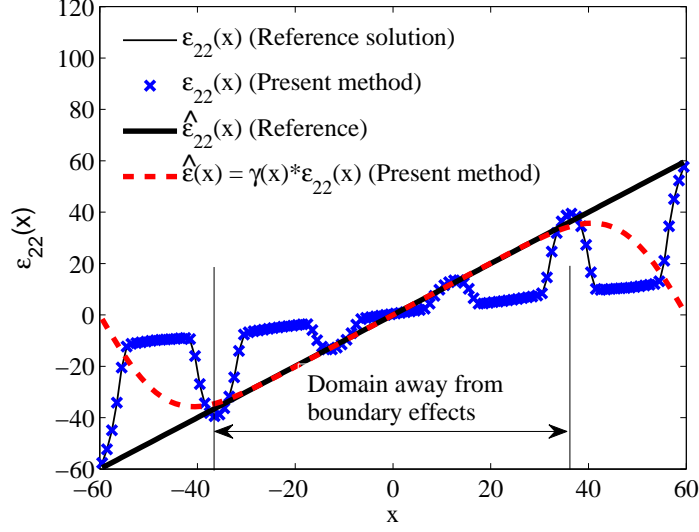
22

Fig. 4. Elementary cell submitted to a linear mesoscopic strain field. Comparison of strain fields through a line $(x, y = 0)$ passing through the inclusions.
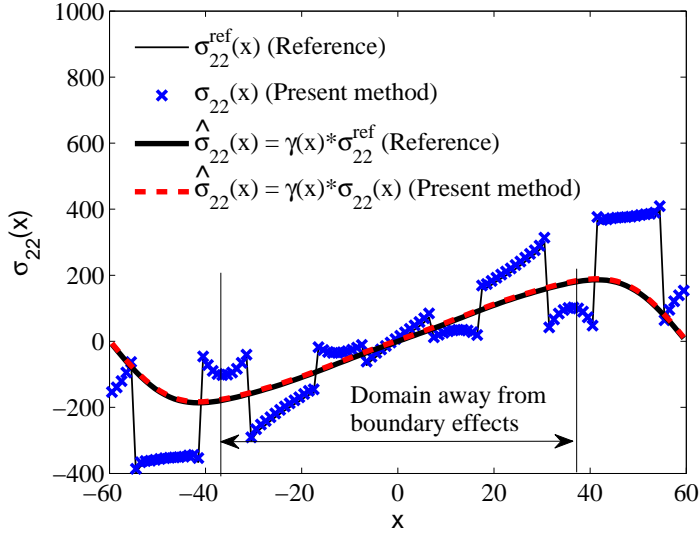

Fig. 5. Elementary cell submitted to a linear mesoscopic strain field. Comparison of stress fields through a line $(x, y = 0)$ passing through the inclusions.

However, as expected, the local reconstructed strain and stress fields perfectly match the computed (reference) solutions, as shown in figures 4 and 5.

In a third test, we now apply a quadratic mesoscopic strain field $\hat{\boldsymbol{\varepsilon}}(\mathbf{x}) = f(x)\mathbf{a}_1 \otimes \mathbf{a}_1$, such that $f(0) = -1/3$, $f(L/2) = 2/3$ and $f(L) = -1/3$. These values have been chosen such that the average of the mesoscopic strain field is zero over the unit cell. The applied mesoscopic strain field is in the form of (69), with $M^p(\mathbf{x})$ being the bilinear shape functions of the 4×4 quadrilateral coarse mesh defined on Ω. The quadratic values are provided at the nodes
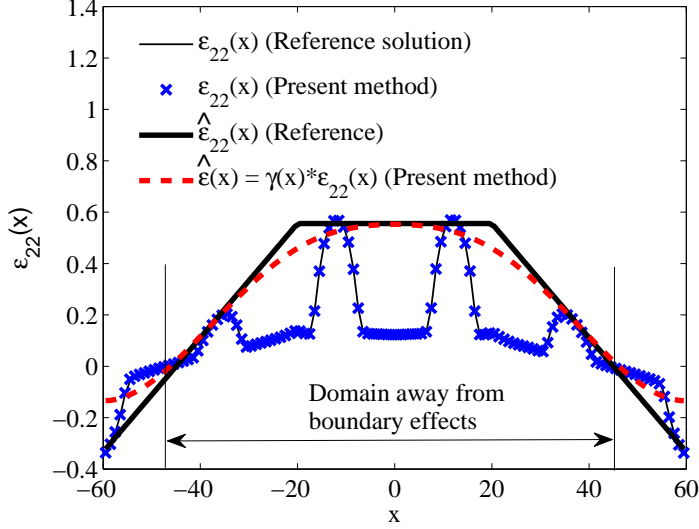
Fig. 6. Elementary cell submitted to a quadratic mesoscopic strain field. Comparison of strain fields through a line $(x, y = 0)$ passing through the inclusions.

of the mesh. We compare the different local, mesoscopic, strain and stress fields computed and reconstructed in figures 6 and 7. In that case, due to the periodicity of the mesoscopic strain field, the boundary effects are less pronounced. They however exist because of the discontinuity in the derivatives of the mesoscopic strain field at the boundaries. Away from the boundaries, the reconstructed local fields match the reference ones with a very good accuracy. Finally, we note in figure 6 a difference between the applied mesoscopic strain $\hat{\varepsilon}(\mathbf{x})$ and the regularized strain $\gamma(\mathbf{x}) * \varepsilon(\mathbf{x})$. This is because the regularization process cannot reproduce the piece-wise polynomial (here bilinear) approximation. One possible further improvement would be to replace the bilinear shape functions by higher order polynomial functions. This will be investigated in future studies.

In the following last test, we check the convergence of the solution with respect to the unit cell size. For this purpose, we consider 4 different unit cells containing 3×3, 5×5, 7×7 and 9×9 inclusions, distributed over a regular square grid as in the illustration of figure 2. The volume fraction is $f = 0.3$ and the properties of the phases are the same as in the previous tests. For each one, we prescribe a mesoscopic strain field $\hat{\varepsilon}(\mathbf{x}) = x\mathbf{a}_2 \otimes \mathbf{a}_2$. We then compute the mesoscopic stress response $\hat{\sigma}_{11}(y)$ along a line $(x, y = 0)$ passing through the center of the cell. Results are presented in figure 8.

We can note that for all cases, the spurious effects of the Gaussian filter remain near the boundaries. However, away from the boundary, we observe that the stress response is convergent with respect to the unit cell size. As opposed to the case when scales are separated, a sufficient number of lattices is necessary to reach convergence even for periodic microstructures because of the artifacts
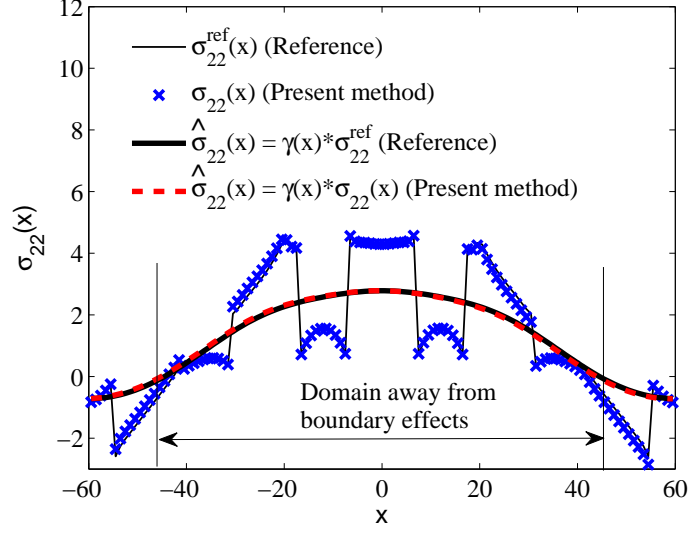
24

Fig. 7. Elementary cell submitted to a quadratic mesoscopic strain field. Comparison of stress fields through a line $(x, y = 0)$ passing through the inclusions.
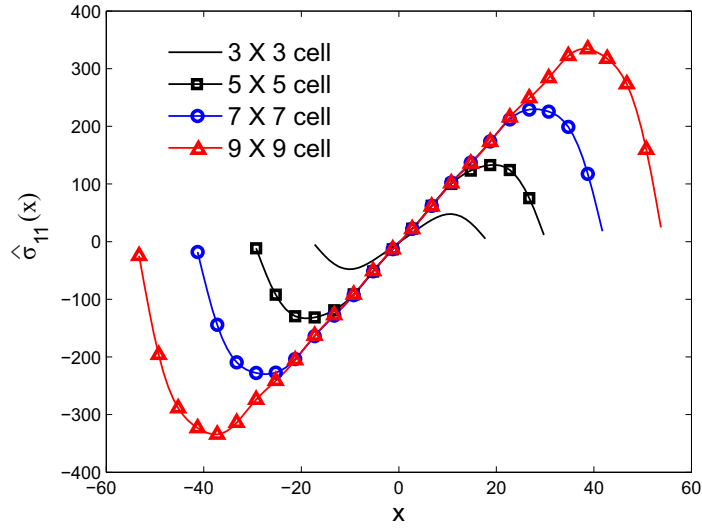

Fig. 8. Mesoscopic stress response with respect to the number of periodic lattice cell in the unit cell subjected to linear mesoscopic strain.

related to the Gaussian filter.

6.2 Validation of the mesoscopic homogenization on a structure problem

The aim of the following example is to compare local and mesoscopic fields in a heterogeneous structure by using the localization tensors computed on a unit cell. As opposed to the previous tests, we solve here a full structure

computation with Dirichlet boundary conditions. The main difficulty is to define a reference solution such that the mesoscopic strain field is known. Here, we adopt the following procedure. We first define a mesoscopic strain field $\hat{\varepsilon}(\mathbf{x})$ which is prescribed on the structure through solving the problem

$$\nabla \cdot (\mathbb{C}(\mathbf{x}) : \boldsymbol{\varepsilon}(\mathbf{x})) = \nabla \cdot \left(\mathbb{C}^0 : \hat{\varepsilon}(\mathbf{x}) \right) \quad \text{in } W, \tag{85}$$

with boundary conditions

$$\mathbf{u}(\mathbf{x}) = \hat{\mathbf{u}}(\mathbf{x}) = \mathcal{I}\left(\hat{\varepsilon}(\mathbf{x}) \right) \quad \text{on} \quad \partial W, \tag{86}$$

where $\mathcal{I}(\hat{\varepsilon})$ is a compatible displacement such that $\boldsymbol{\varepsilon}\left(\hat{\mathbf{u}}(\mathbf{x}) \right) = \hat{\varepsilon}(\mathbf{x})$. We can verify that in the case $\mathbb{C}(\mathbf{x}) = \mathbb{C}^0$ then $\hat{\mathbf{u}}(\mathbf{x})$ is statically and kinematically compatible and is then also the solution for all $\mathbf{x} \in \Omega$. In that case, $\boldsymbol{\varepsilon}(\mathbf{x}) = \hat{\varepsilon}(\mathbf{x})$. However, for a heterogeneous structure, this is not the case and the computed strain field obviously does not satisfy condition (8). To construct the reference mesoscopic solution, we then fit the obtained local strain field with a tensor function known in an analytical form, as shown below.

6.2.1 Heterogeneous structure subjected to a bending moment

In this example, the strain field is chosen as $\hat{\varepsilon}(\mathbf{x}) = xy/\alpha \mathbf{a}_1 \otimes \mathbf{a}_1$, which corresponds to a bending mode of the structure, with Dirichlet boundary conditions given by

$$\mathbf{u}(\mathbf{x}) = \frac{x^2 y}{2\alpha} \mathbf{a}_1 - \frac{x^3}{6\alpha} \mathbf{a}_2. \tag{87}$$

We choose $\alpha = 500$, the dimensions along x and y are $L = 270$ mm and $H = 270$ mm, respectively, and the characteristics of the microstructure (both material and geometrical properties) are identical to those of the previous example. The properties of $\mathbb{C}^0$ are those of an isotropic elastic medium with $\lambda^0 = 1$ and $\mu^0 = 1$ GPa. The heterogeneous structure is composed of 15×15 inclusions centered in square periodic cells, as depicted in figure 9 (b). The magnified deformation of the structure is depicted in figure 10. We then fit the local strain field with a mesoscopic strain field in the form

$$\hat{\varepsilon}_{kl}^{ref}(\mathbf{x}) = \sum_{i,j} \frac{1}{2} (\alpha_{ij} + \beta_{ij} x + \gamma_{ij} y + \epsilon_{ij} xy) \left(\mathbf{a}_k \otimes \mathbf{a}_l + \mathbf{a}_l \otimes \mathbf{a}_k \right). \tag{88}$$

The parameters of the fitting are given in Table 2.

The unit cell for the problem is the same as the one used in the previous examples.

Table 2
Coefficients of the mesoscopic strain model in example 6.2.1, rigid inclusions.

α_{11}	5.806	β_{11}	-0.0377	γ_{11}	0.0363	ϵ_{11}	0.0018
α_{22}	2.1157	β_{22}	0.0020	γ_{22}	-0.0141	ϵ_{22}	0.0000
α_{12}	6.7700	β_{12}	-0.0081	γ_{12}	-0.0371	ϵ_{12}	0.0000

Fig. 9. (a) Applied mesoscopic strain field; (b) heterogeneous structure; (c) unit cell.

In figure 11, we compare the local strain fields obtained by directly solving the structure problem and by using reconstructed local fields through $\hat{\mathbb{A}}^p(\mathbf{x})$, and the values of the reference mesoscopic strain field at the nodes of the coarse grid on the unit cell, which is still here a 4×4 grid. For this purpose, the solution $\hat{\varepsilon}_{11}(x)$ is plotted on a line $(x, y = H/2)$ passing through the inclusions. In addition, we plot the reference mesoscopic strain and the reconstructed mesoscopic strain field, obtained by a filter of the reconstructed strain field on the unit cell. We can observe that the proposed framework provides a good approximation of both local and mesoscopic strain fields, even if some discrepancies exist (small artifacts on $\gamma(x) * \varepsilon_{11}(x)$, red dotted line in figure 11), due to the boundary effects of the filtering numerical procedure on one hand, and to the definition of the reference solution itself.

In a second example, we consider a structure whose dimensions along x and y are $L = 360$ mm and $H = 120$ mm, respectively. The microstructure is comparable with the one depicted in figure 9, but is composed of 15×5 inclusions with highly compliant properties $\lambda_{inc} = \mu_{inc} = 10^{-6}$ GPa to model pores. The properties of the matrix are $\lambda_{mat} = \mu_{mat} = 1$ GPa. The same
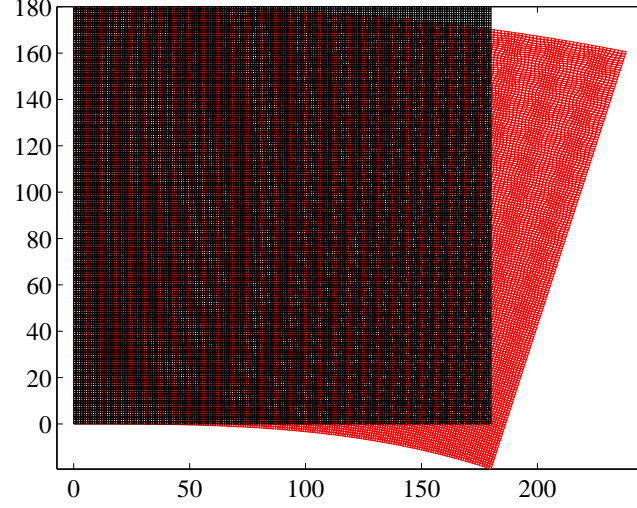
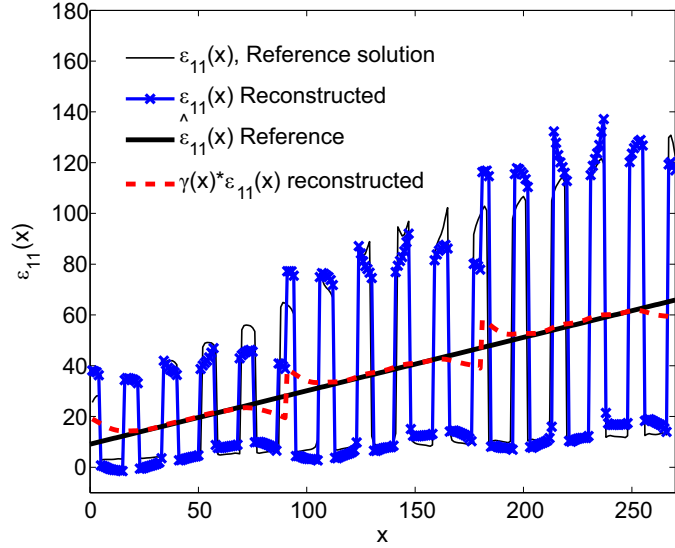Fig. 10. Deformation of the structure, initial (black) and deformed (red) meshes.

Fig. 11. Comparison of structure and homogenized solutions, structure in bending with rigid inclusions.

loading as in the previous example is prescribed. The reference solution for the mesoscale strain field is constructed as in the previous example, by fitting the full solution with the analytical form (88). The found coefficients are provided in Table 3.

Results are presented in figure 12. Here again, the results are in satisfying agreement with the reference solution.

Table 3
Coefficients of the mesoscopic strain model in example 6.2.1, porous structure.

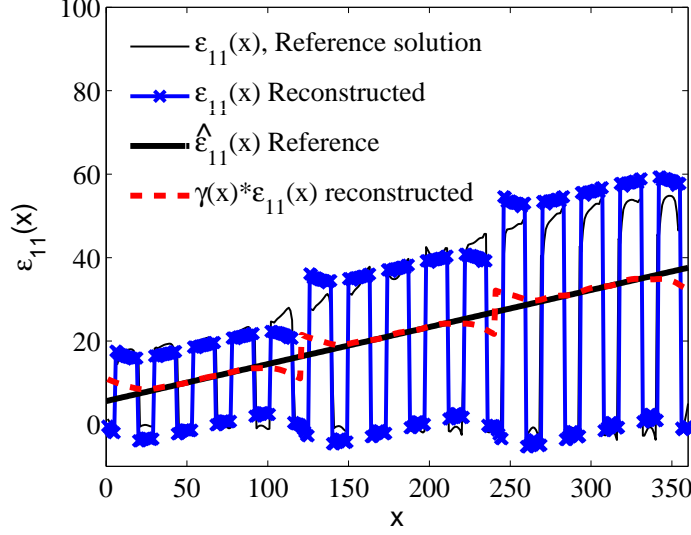| α_{11}	4.3448	β_{11}	0.0213	γ_{11}	-0.0231	ϵ_{11}	0.0019
α_{22}	1.2525	β_{22}	-0.0209	γ_{22}	0.0200	ϵ_{22}	-0.0003
α_{12}	8.9135	β_{12}	-0.1350	γ_{12}	-0.0034	ϵ_{12}	0.0000

Fig. 12. Comparison of structure and homogenized solutions, structure in bending with pores.

6.2.2 Heterogeneous structure subjected to heterogeneous body forces

In this next example, a heterogeneous structure containing 15×5 inclusions, as depicted in figure 13 is studied. An oscillating mesoscopic strain field is prescribed on the structure through body forces, like those which might arise in a dynamic problem. The characteristic period is not much larger than the characteristic dimension of the inclusions, and the scales cannot be separated. The microstructure is the same as in the previous example and the unit cell is the one depicted in figure 2. The elastic parameters of matrix and inclusions are $\lambda_{mat} = \mu_{mat} = 1$ GPa and $\lambda_{inc} = \mu_{inc} = 10$ GPa, respectively. The dimensions along x and y are $L = 180$ mm and $H = 60$ mm, respectively. In this example, the mesoscopic strain field is given by

$\hat{\varepsilon}(\mathbf{x}) = sin(\pi x/(3L))\mathbf{a}_1 \otimes \mathbf{a}_1$, modeling the effects of a dynamic body forces, with Dirichlet boundary conditions given by

$$\mathbf{u}(\mathbf{x}) = -\frac{3L}{\pi}cos(x*\pi/(3L))\mathbf{a}_1 \tag{89}$$

In this case, the resulting microscopic strain field is fitted with a reference
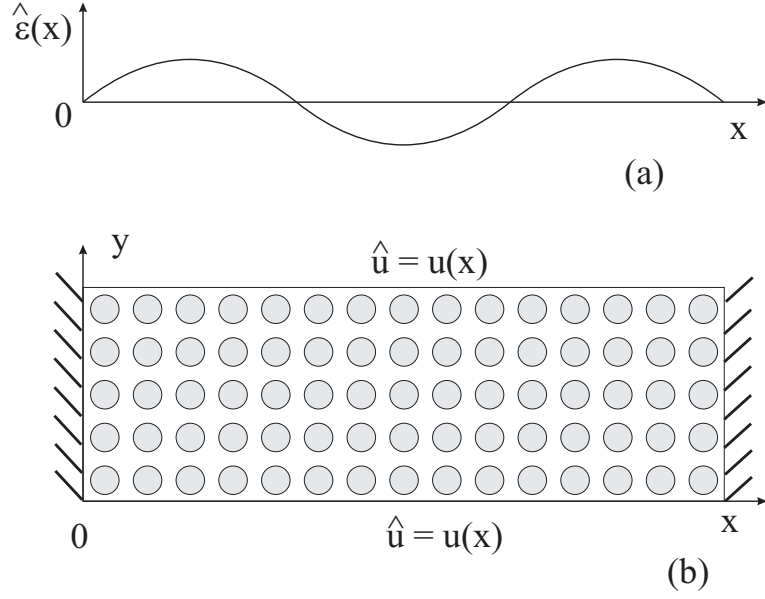
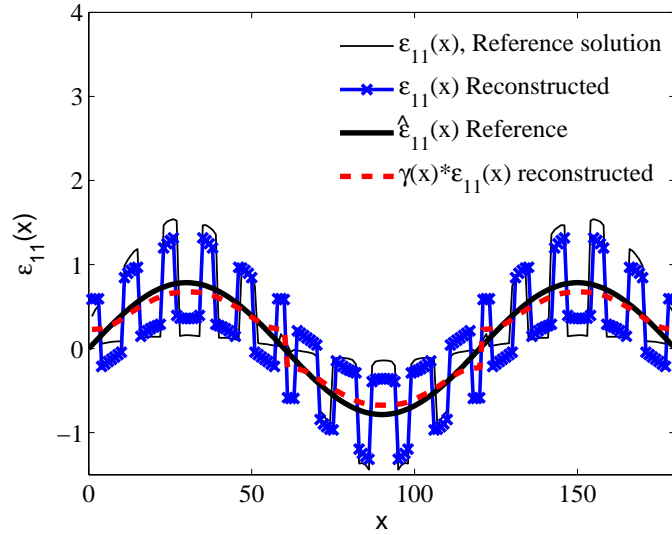Fig. 13. (a) Applied mesoscopic strain field; (b) heterogeneous structure;

Fig. 14. Comparison of structure and homogenized solutions

mesoscopic strain field in the form

$$\hat{\boldsymbol{\varepsilon}}^{ref}(\mathbf{x}) = \alpha_{11} sin(\pi x/(3L))\mathbf{a}_1 \otimes \mathbf{a}_1 \qquad (90)$$

The fitting procedure gives $\alpha_{11} = 0.6680$. Results comparing local and mesoscopic strain field for reference and computed solution are provided in figure 14. Even though this approximation is more suitable to infinite bodies, due to the boundary effects related to the Gaussian filter, we can note that it provides here again satisfying agreement with respect to the reference solution in a finite domain, even near the clamped edge.

7 Conclusion

A framework for homogenization of linearly, heterogeneous materials in the case of non-separated scales has been proposed. The mesoscopic strain and stress fields are defined as the action of a low-pass filter which smoothes the fine scale fluctuations. Then, the localization problem defined on the elementary cell can be formulated as an elasticity problem with non-uniform eigenstrains. The mesoscopic stress and strain fields can be related to each other by using a linear operator, which appears to be nonlocal. As opposed to the Eringen model [11–13], the present model is fully microstructurally founded and naturally takes into account the effects of any kind of heterogeneities and constitutes a *consistent nonlocal homogenization framework*. A discrete theory is provided to compute the mesocopic stress-strain relationship numerically by means of computations on the unit cell. In this paper, we have focused on presenting the overall theory. The numerical details of finite element implementation, both related to the resolution at the microscopic and at the mesoscopic scales, will be provided in a forthcoming paper. Another way of improvement of the methodology will consist in defining alternative regularization procedures which do not introduce spurious boundary effects.

8 Appendices

8.1 Appendix A: Green function of the mesoscale localization problem

The Green function in Eq. (10) must verify:

$$\left[C_{ijkl}(\mathbf{x})\hat{\Gamma}_{klmn}(\mathbf{x},\mathbf{y})\right]_{,j} = -\left[C_{ijkl}(\mathbf{x})\mathcal{D}_{kl}^{mn}(\mathbf{x}-\mathbf{y})\right]_{,j} \tag{91}$$

and

$$\gamma(\mathbf{x}) * \Gamma_{klmn}(\mathbf{x},\mathbf{y}) = \mathcal{D}_{kl}^{mn}(\mathbf{x}-\mathbf{y}) \tag{92}$$

with periodic boundary conditions and:

$$\mathcal{D}_{kl}^{mn}(\mathbf{x}-\mathbf{y}) = \frac{\delta(\mathbf{x}-\mathbf{y})}{2}\left[\mathbf{a}_m \otimes \mathbf{a}_n + \mathbf{a}_n \otimes \mathbf{a}_m\right]_{kl}. \tag{93}$$

Eq. (71) is a regularized and discretized version of Eq. (91), taking into account the condition (92) by the procedure described in section 2.3.1.

31

8.2 Appendix B: Gain related to a Gaussian field

Let $f(x) = f e^{i\hat{\omega}x}$ a scalar oscillating function with amplitude f and characteristic frequency $\hat{\omega}$. A closed-form expression of the convolution product with a Gaussian function $\gamma(x)$ of the form (3) can be established as

$$\gamma_\alpha(x) * f(x) = f e^{-\frac{\alpha^2 \hat{\omega}^2}{4}} e^{i\hat{\omega}x} = f_1(x). \tag{94}$$

Applying again the Gaussian filter yields

$$\gamma_\alpha(x) * \gamma_\alpha(x) * f(x) = f e^{-\frac{\alpha^2 \hat{\omega}^2}{2}} e^{i\hat{\omega}x} = f_2(x). \tag{95}$$

The ratio of the signal output to the signal input is given by

$$\frac{|f_2(x)|}{|f_1(x)|} = \frac{e^{-\frac{\alpha^2 \hat{\omega}^2}{2}}}{e^{-\frac{\alpha^2 \hat{\omega}^2}{4}}} = e^{-\frac{\alpha^2 \hat{\omega}^2}{4}} = h(\alpha, \hat{\omega}). \tag{96}$$

The parameter $h \simeq 1$ if $\frac{1}{\alpha} >> \hat{\omega}$. An illustration of this approximation is provided in figure 15. The signal $\varepsilon(x)$ is the same as the one defined in section 2.1.

In figure 16, the gain of the signal is plotted versus $\alpha.\hat{\omega}$ when the Gaussian filter is applied once and twice.

8.3 Appendix C: One dimensional problem with prescribed linear mesoscopic strain field and zero strain average

Let us consider a heterogeneous one-dimensional problem defined over a domain $\Omega = [-a, a]$, characterized by elastic properties $C(x) = C_1$ for $x \in [-b, b]$, $b < a$, and $C(x) = C_2$ for $x \notin [-b, b]$. In one dimension, problem (30) reduces to

$$\frac{d}{dx}\left(E(x)\frac{du(x)}{dx}\right) = -\frac{d}{dx}\left(C(x)\hat{\varepsilon}(x)\right) \tag{97}$$

with $u(x)$ such that $e^1(x) = \frac{du(x)}{dx}$ and $u(x)$ periodic on $x = -a$ and $x = a$. For example, for $\hat{\varepsilon}(x) = \alpha x$, $\alpha \in \mathbb{R}$, the displacement solution is given by

$$u(x) = -\frac{\alpha x^2}{2} + A_i x + B_i \tag{98}$$

where the constants A_i, B_i can be determined by expressing the continuity of displacements and traction $\sigma(x) = C(x)\left[e(x) + \hat{\varepsilon}(x)\right]$ at the interfaces $x = -b$
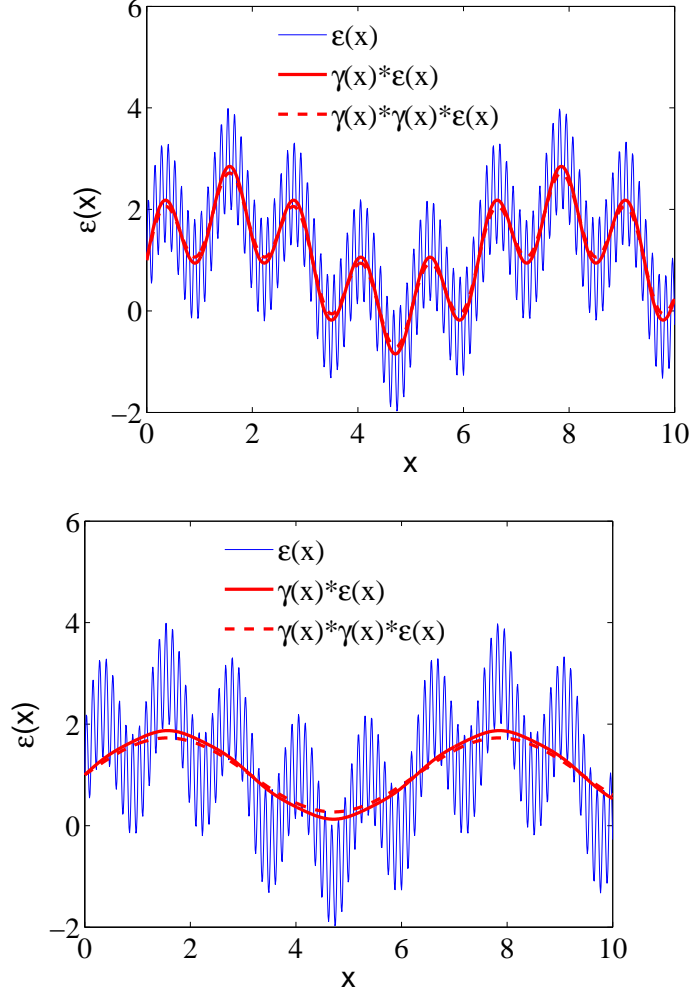
Fig. 15. Illustration of the approximation (15) for (a) $\alpha/\lambda_{min} = 1/20$ and (b) $\alpha/\lambda_{min} = 1$

and $x = b$ and the periodicity of the solution on the boundary $x = -a$ and $x = a$. The resulting linear system of equations yields $A_i = 0$, $i = 1, 2, 3$ which produces the trivial solution $e^1(x) = -\alpha x$. The regularization of a linear function with a Gaussian filter leaves it unchanged, which gives $\gamma(x) * e^1(x) = -\alpha x = e^1(x)$. Finally we obtain

$$\tilde{\varepsilon}(x) = e^1(x) - \gamma(x) * e^1(x) = 0. \tag{99}$$

Note that this artefact only occurs in the 1D case, as shown in the 2D numerical examples of section 6.
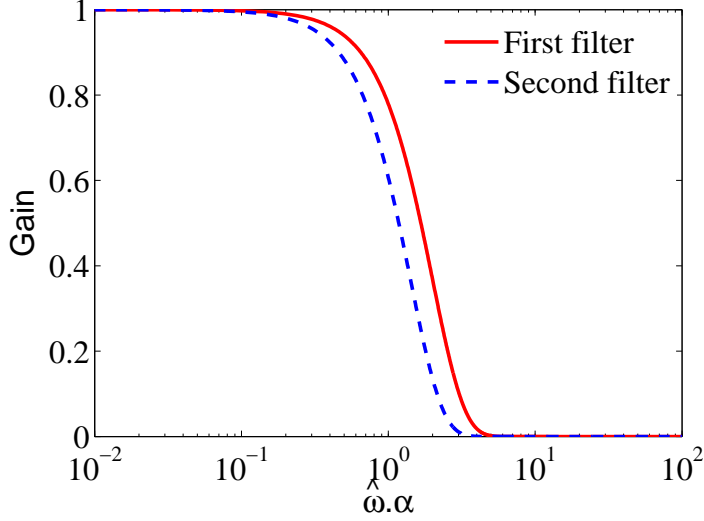
33

Fig. 16. Illustration of the signal attenuation when applying the Gaussian filter as a function of $\hat{\omega}\alpha$.

8.4   Appendix D: Convergence of the iterative scheme (28)

It was observed during our numerical tests that the iterative scheme (28) was always convergent, contrarily for example to the classical iterative scheme used within FFT numerical solutions which depends strongly of a "reference medium" (see e.g. a discussion in [34]). The iterative scheme in (28) involves a filtering nonlocal operator and the method employed for studying the convergence of FFT iterative scheme cannot be used. This appendix proves the unconditional convergence of the iterative scheme (28).

Let us consider the iterative scheme of (28), where $\mathbf{e}^{k+1}$ is sought with periodicity boundary conditions. This iterative scheme can be written as:

$$\mathbb{L}(\mathbf{e}^{k+1}) = \mathbf{f} + \nabla \cdot \left(\mathbb{C}(\mathbf{x}) : \gamma_\alpha(\mathbf{x}) * \mathbf{e}^k(\mathbf{x}) \right), \tag{100}$$

where $\mathbb{L}$ is the differential operator $\mathbb{L}(\cdot) = \nabla \cdot (\mathbb{C}(\mathbf{x}) : \cdot)$ and $\mathbf{f} = -\mathbb{L}(\hat{\boldsymbol{\varepsilon}})$. For periodic boundary conditions on the solution, the boundary problem admits a unique solution $\mathbf{e}^{k+1}$, which may be considered as given by the inverse operator $\mathbb{L}^{-1}$, leading to:

$$\mathbf{e}^{k+1} = \mathbb{L}^{-1}(\mathbf{f}) + \mathbb{L}^{-1}(\nabla \cdot \left(\mathbb{C}(\mathbf{x}) : \gamma_\alpha(\mathbf{x}) * \mathbf{e}^k(\mathbf{x}) \right)). \tag{101}$$

The iterative process is related to the eigenvalues of the recursive operator $\mathbb{A}(\cdot) = \mathbb{L}^{-1}(\nabla \cdot (\mathbb{C}(\mathbf{x}) : \gamma_\alpha(\mathbf{x}) * \cdot))$.

34

Let us now introduce the Fourier basis of the fields of strain tensors whose generic element can be written:

$$\mathbf{g}_{\xi,l} = \mathbf{e}_l.e^{i\xi.\mathbf{x}}, \tag{102}$$

where $\mathbf{e}_l$ with $l = 1..6$ constitute a basis of constant symmetrical strain tensors and ξ are wave vectors along the reciprocal lattice of the periodic cell.

From Appendix B, one has:

$$\gamma_\alpha(\mathbf{x}) * \mathbf{g}_{\xi,l}(\mathbf{x}) = e^{-\frac{\alpha^2}{4}\|\xi\|^2} \mathbf{g}_{\xi,l}(\mathbf{x}) \tag{103}$$

As a consequence, it yields:

$$\mathbb{A}(\mathbf{g}_{\xi,l}) = e^{-\frac{\alpha^2}{4}\|\xi\|^2} \mathbb{L}^{-1}(\nabla \cdot (\mathbb{C}(\mathbf{x}) : \mathbf{g}_{\xi,l})) = e^{-\frac{\alpha^2}{4}\|\xi\|^2} \mathbf{g}_{\xi,l}. \tag{104}$$

This proves that the components of the Fourier basis are eigenfunctions of the iterative operator $\mathbb{A}$ with eigenvalues comprised between 0 and 1, leading to the unconditional convergence of the iterative operator.

References

[1] Bensoussan, A., Lions, J.-L., Papanicolaou, G.C., 1978. Asymptotic Analysis for periodic Structures. North-Holland, Amsterdam.

[2] Beran, M.J., McCoy, J.J., 1970. Mean-field variations in a statistical sample of heterogeneous linearly elastic solids. Int. J. Solids Struct. 6, 1035–1054.

[3] Boutin, C., 1996. Microstructural effects in elasticcomposites. Int. J. Solids Struct. 33(7), 1023–1051.

[4] Bouyge, F., Jasiuk, I., Ostoja-Starzewski, M., 2001. A micromechanically based couple-stres model of an elastic two-phase composite. Int. J. Solids Struct. 38, 1721–1735.

[5] Bouyge, F., Jasiuk, I., Ostoja-Starzewski, M., 2002. A micromechanically based couple-stres model of an elastic orthotropic two-phase composite. Eur. J. Mech. A. 21, 46548.

[6] de Felice, G., Rizzi, N., 2001. Homogenization formaterials with microstructure. In Recent Advances in Solids/Structures and Application of Metallic Materials. vol. PVP-vol. 369. ASME: New York, 1997; 33–38.

[7] Diener, G., Raabe, C.H., Weissbarth, J., 1981. Bounds for the nonlocal effective properties of random media. J. Mech. Phys. Solids 29(3), 181–198.

[8] Diener, G., Raabe, C.H., Weissbarth, J., 1982. Bounds for the non-local effective properties of random media II. J. Mech. Phys.Solids 30(5), 305–322.

[9] Diener, G., Raabe, C.H., Weissbarth, J., 1984. Bounds on the non-local effective elastic properties of composites. J. Mech. Phys. Solids 32(1), 21–39.

[10] Drugan, W.J., Willis, J.R., 1996. A micromechanics-based nonlocal constitutive equation and estimates of representative volume element size for elastic composites. J. Mech. Phys.Solids 44 (4), 497–524.

[11] Eringen, A.C., 1972. Nonlocal polar elastic continua. Int. J. Engng. Sci. 10, 1–16.

[12] Eringen, A.C., 1972. Linear theory of nonlocal elasticity and dispersion of plane waves. Int. J. Engng. Sci. 10, 425–435.

[13] Eringen, A.C., 1976. Nonlocal micropolar field theory. In: Eringen, A.C. (Ed.), Continuum physics, vol. 4. Academic Press, New York, pp. 205–267.

[14] Eringen, A.C., Edelen, D.G.B., 1972. On nonlocal elasticity. Int. J. Engng Sci. 10, 233–248.

[15] Eringen, A.C., Kim, B.S., 1974. Stress concentration at the tip of a crack. Mesh. Res. Commun. 1, 233–237.

[16] Eringen, A.C., Speziale, C.G., Kim, B.S., 1977. Crack-tip problem in non-local elasticity. J. Mech. Phys. Solids. 25, 339–355.

[17] Eringen, A.C., 1983. On Differential Equations of Nonlocal Elasticity and Solutions of Screw Dislocation and Surface Waves. J. Appl. Phys. 54, 4703–4710.

[18] Fleck, N.A., Hutchinson, J.W., 1997. Strain gradient plasticity. Adv. Appl. Mech. 33, 295–361.

[19] Forest, S., Sab, K., 1998. Cosserat overall modelling of heterogeneous materials, 1998. Mech. Res. Commun. 25(4), 449–454.

[20] Forest, S., Dendievel, R., Canova, G.R., 1999. Estimating the overall properties of heterogeneous Cosserat materials. Model. Simul. Mater. Sci. Eng. 7, 829–840.

[21] Forest, S., Pradel, F., Sab, K., 2001. Asymptotic analysis of heterogeneous Cosserat media. Int. J. Solids Struct. 38, 4585–4608.

[22] Furmanski P., 1997. Heat condution in composites: Homogenization and macroscopic behavior. Appl. Mech. Rev. 50, 327–356.

[23] Gambin, B., Kroener, E., 1989. High order terms in the homogenized stress-strain relation of periodic elastic media. Phys. Status Solidi B - Basis Solid State Phys. 151, 513–519.

[24] Gao, J., 1999. An asymetric theory of nonlocal elasticity–part 2. Continuum field. Int. J. Solids. Struct. 36, 2959–2971.

[25] Green, A.E., Rivlin, R.S., 1964. Multipolar continuum mechanics. Arch. Rat. Mech. Anal. 17, 113–147.

[26] Koiter, W.T., 1964. Couple-stress in the theory of elasticity, 1964. Proceedings of the Koninklijke Nederlandse Akademie vanWetenshappen Series B, 64(1), 17–44.

[27] Kouznetsova, V., Geers, M.G.D., Brekelmans, W.A.M., 2002. Multi-scale constitutive modeling of heterogeneous materials with gradient enhanced computational homogenization scheme. Int. J. Numer. Methods Eng. 54, 1235–1260.

[28] Kouznetsova, V., Geers, M.G.D., Brekelmans, W.A.M., 2004. Multi-scale second-order computational homogenization of multi-phase materials: a nested finite element solution strategy. Comput. Meth. Appl. Mech. Eng. 193, 5525–5550.

[29] Kröner, E., Statistical Continuum Mechanics: Course held at the Department of General Mechanics, October 1971. Springer-Verlag, Wien, 1972.

[30] Kröner, E., 1967. Elasticity theory of materials with long-range cohesive forces. Int. J. Solids Struct., 3, 731–742.

[31] Luciano, R. Willis, J.R., 2000. Bounds on non-local effective relations for random composites loaded by configuration-dependent body force, J. Mech. Phys., 48(9), 1827–1849.

[32] Mindlin, R.D., 1964. Micro-structure in linear elasticity. Arch. Rat. Mech. Anal. 16, 51–78.

[33] Mindlin, R.D., Eshel, N.N., 1968. On first gradient theory in linear elasticity. Int. J. Solids Struct. 4, 109–124.

[34] Monchiet, V., Bonnet, G., 2012. A polarization-based FFT iterative scheme for computing the effective properties of elastic composites with arbitrary contrast. Int. J. Numer. Meth. Engng. 89, 1419–1436.

[35] Moës, N., Cloirec, M. Cartraud, P. Remacle, J.-F., 2003. A computational approach to handle complex microstructure geometries. Comput. Meth. Appl. Mech. Eng. 192, 3163–3177.

[36] Moulinec, H., Suquet, P., 1994. A fast numerical method for computing the linear and nonlinear properties of composites. Comptes R. Acad. Sc. 318, 1417–1423.

[37] Ostoja-Starzewski, M., Boccara, S.D., Jasiuk, I., 1999. Couple-stress moduli and characteristic length of a two-phase composite. Mech. Res. Commun. 26(4), 387–396.

[38] Polizzotto, C., 2001. Nonlocal elasticity and related variational principles. Int. J. Solids Struct. 38, 7359–7380.

[39] Sanchez-Palencia, E., 1980. Nonhomogeneous media and vibration theory. Lect. Notes Phys. 127.

[40] Smyshlyaev, V.P., Cherednichenko, K.D., 2000. Onrigorous derivation of strain gradient effects in the overall behaviour of periodic heterogeneous media. J. Mech. Phys. Solids. 48, 1325–1357.

[41] Suquet, P., Local and global aspects in the mathematical theory of plasticity. In Plasticity Today: Modelling, Methods and Applications, Sawezuk A., Bianchi G. (Eds.) Elsevier Applied Science Publishers: London, 1985; 279–310.

[42] Suquet, P., 1987. Homogenization techniques for composites media. Lecture Notes in Physics, 1987, 272, Springer-Verlag, New-York.

[43] Toupin, R., 1962. Theories of elasticity with couple-stress. Arch. Rat. Mech. Anal. 11(1), 385–414.

[44] Toupin, R., 1964. Theories of elasticity with Couple-stress. Arch. Rat. Mech. Anal. 17(2), 85–112.

[45] Tran, T.-H., Monchiet, V., Bonnet, G., 2012. Amicromechanics-based approach for the derivation of constitutive elastic coefficients of strain-gradient media. Int. J. Solids. Struct. 49, 783–792.

[46] Triantafyllidis, N., Bardenhagen, S., 1996.The influence of scale size on the stability of periodic solids and the role of associated higher order gradient continuum models. J. Mech. Phys. Solids 44, 1891–1928.

[47] Willis, J.R., 1983. The overall elastic response of composite materials. J. Appl. Mech. 50, 1202–1209;

[48] Yuan, X., Tomita, Y., 2008. A micromechanical approach of nonlocal modeling for media with periodic microstructures. Mech. Res. Commun. 35, 126133.